Modeling of porous materials consisting of isotropic and anisotropic matrix and implications on deformation localization

Kostas Danas

CNRS & Ecole Polytechnique, France

Joint Work with:

Armel Mbiakop & Andrei Constantinescu (Ecole Polytechnique)

Nick Aravas (University of Thessaly, Greece)

IUTAM Symposium: Ductile Fracture and Localization

Paris, France

20th March 2015

Cyclic loading of a porous unit-cell

Void shapes as a result of fabrication

Aluminium Alloy, A319, Lost Foam Casting

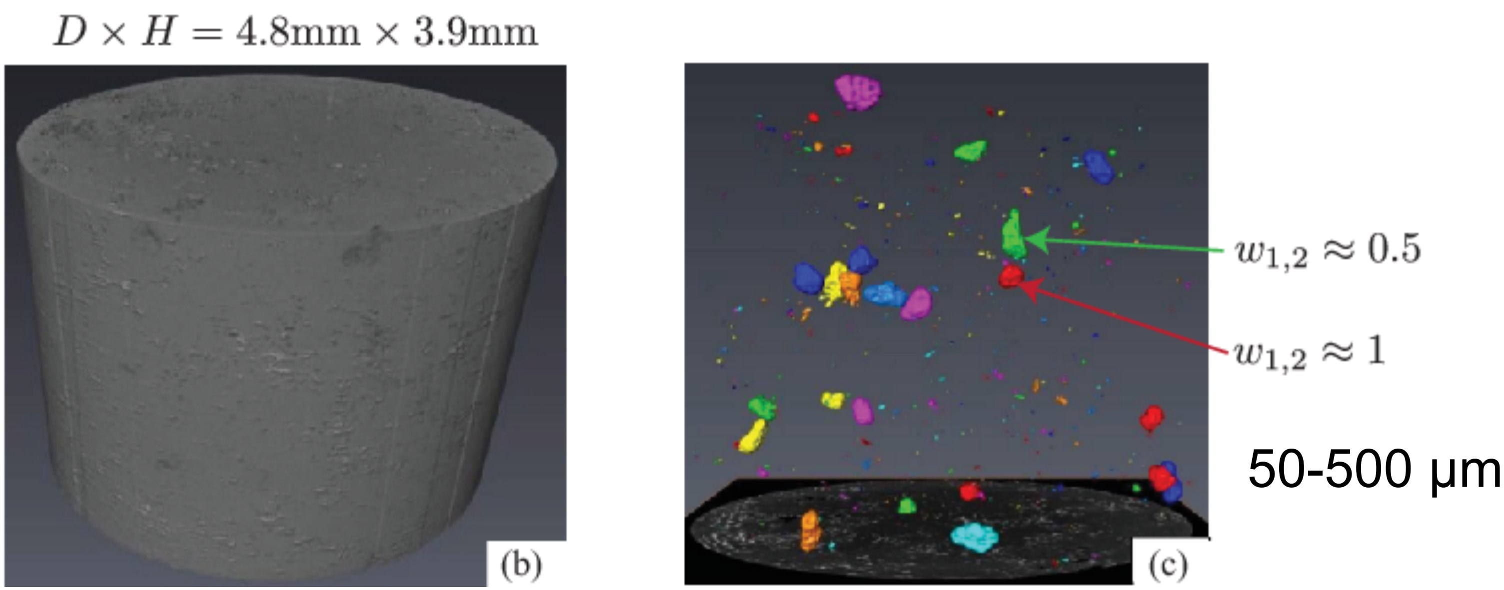

[Limodin et al., 2013]

- 3-D close up of coalescing elongated voids in the L-S plane in one column

Courtesy of Limodin and Charkaluk

The geometry of the unit-cell

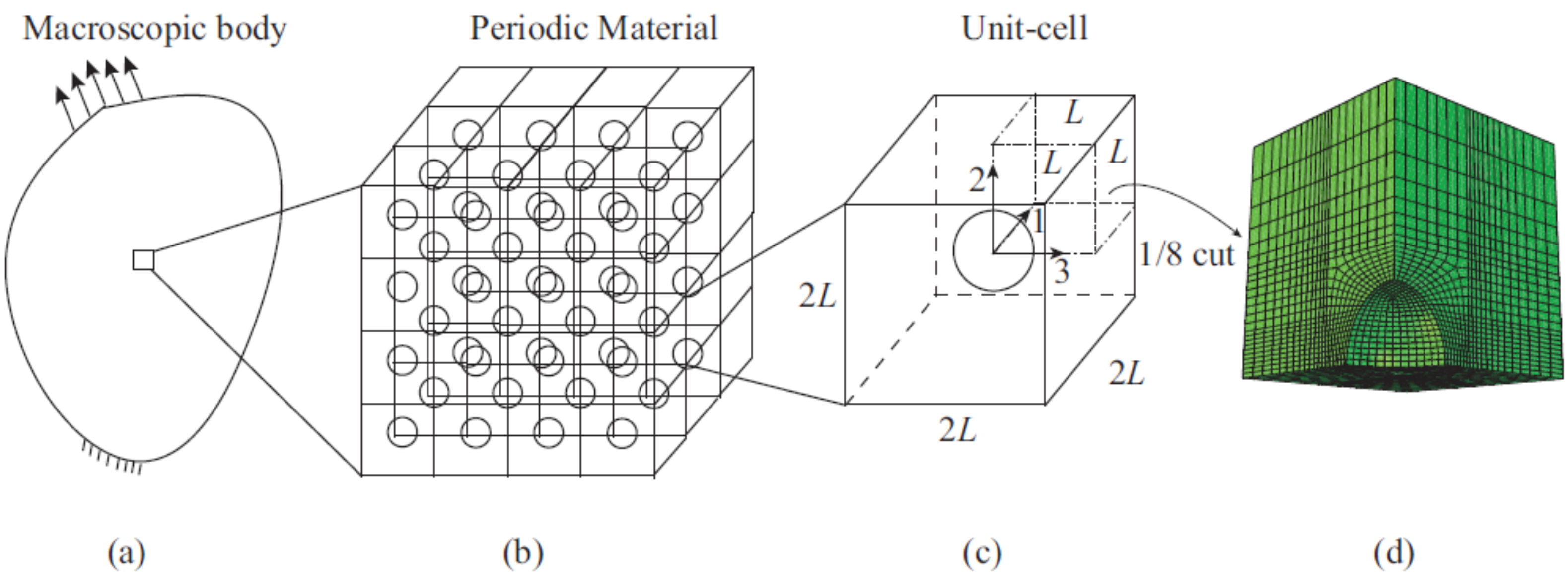

Periodic boundary conditions

$$\sigma \cdot n \quad \text{anti} - \text{periodique}, \quad v = D \cdot x + v^*, \quad v^* \quad \text{periodique}$$

Mbiakop et al., EJMSOL/A, 2015

Cyclic loading at constant Xs and Lode

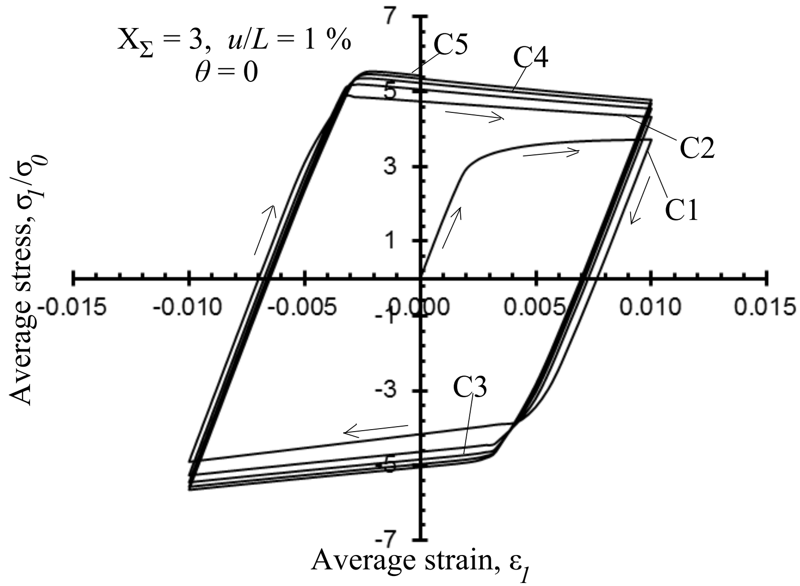

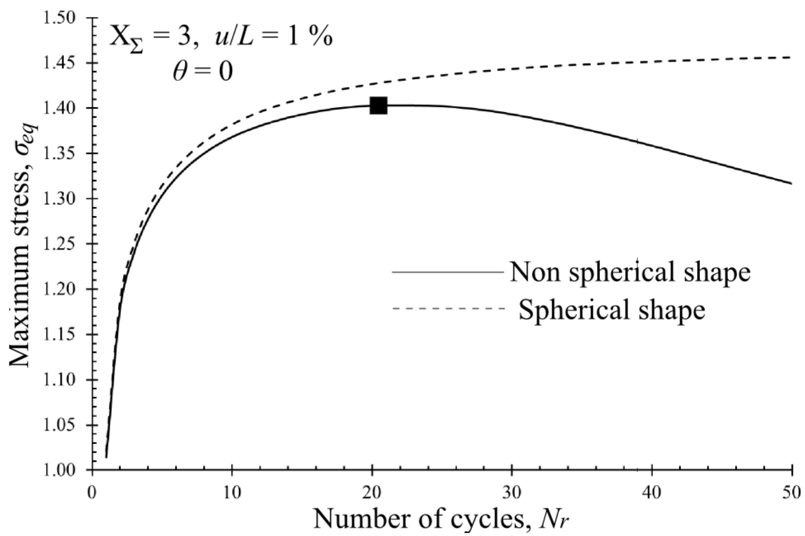

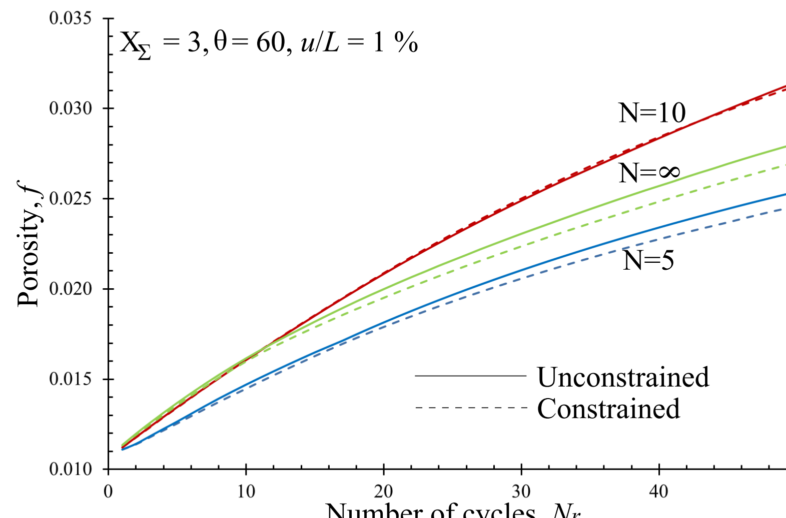

Mbiakop et al., EJMSOL/A, 2015

FEM simulations: Qualitative results

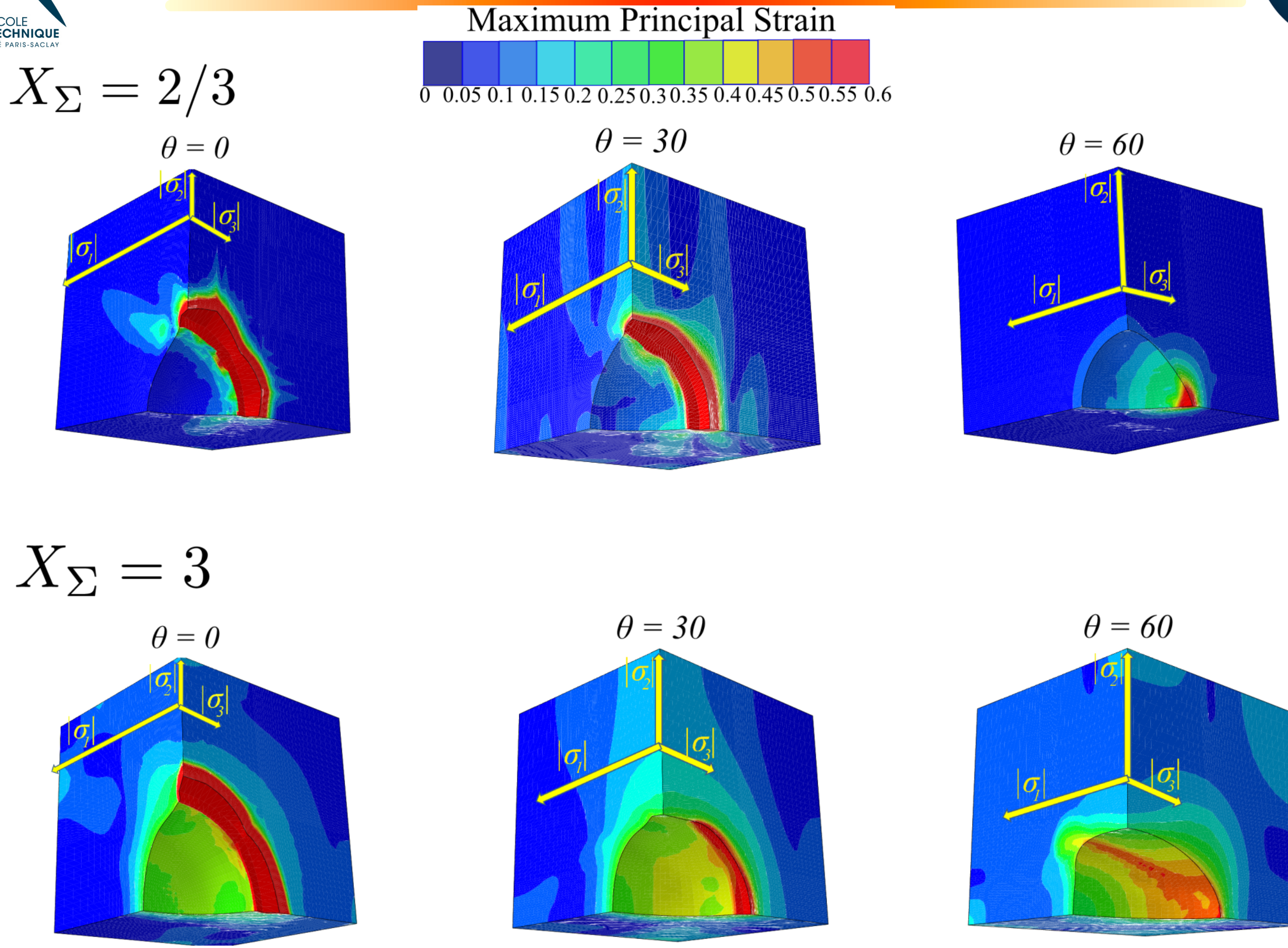

Mbiakop et al., EJMSOL/A, 2015

Effect of kinematic hardening

$$\dot{X}^{(1)} = q_h C_1 D^p_M, \quad \dot{X}^{(2)} = q_h C_2 D^p_M - \gamma_2 \Delta\epsilon^p X^{(2)}$$

$$\longrightarrow X_\Sigma = 3,\ \theta = 0$$

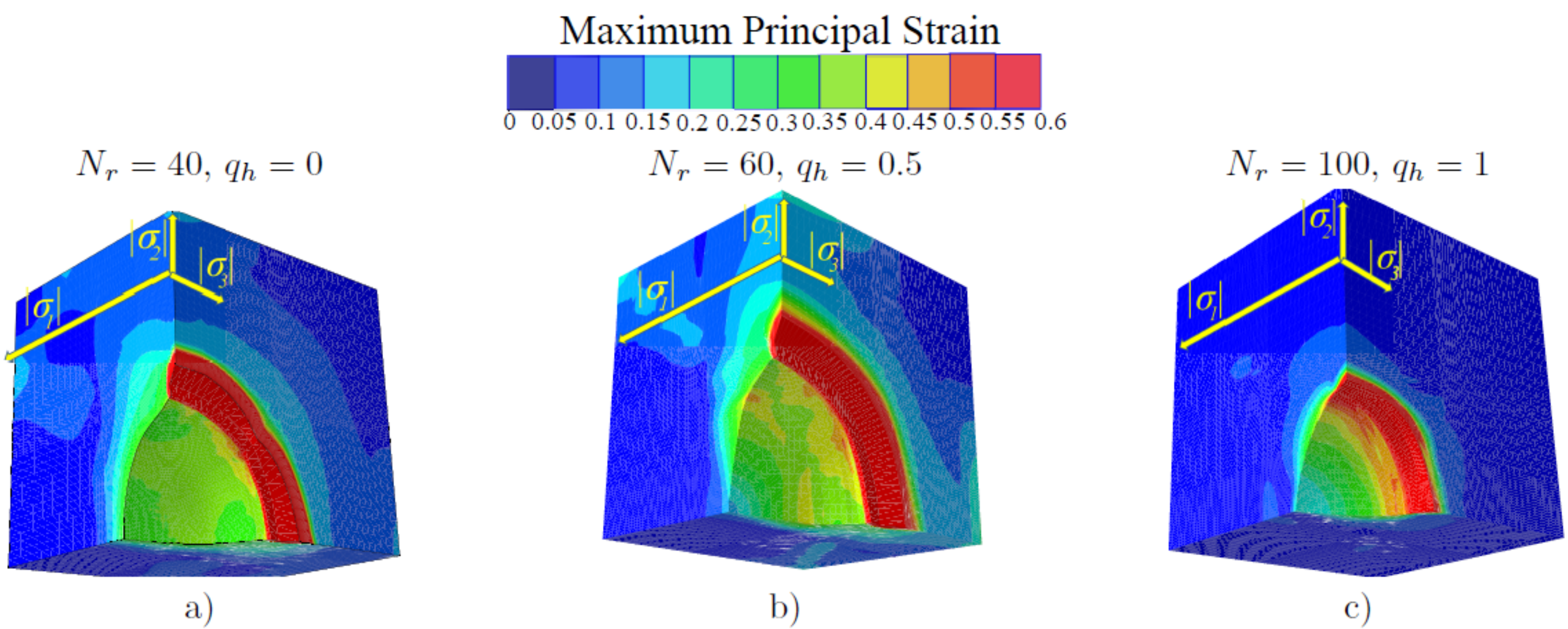

Mbiakop et al., EJMSOL/A, 2015

Effect of initial void shape

$$X_\Sigma = 3, \theta = 60, u/L = 1\%$$

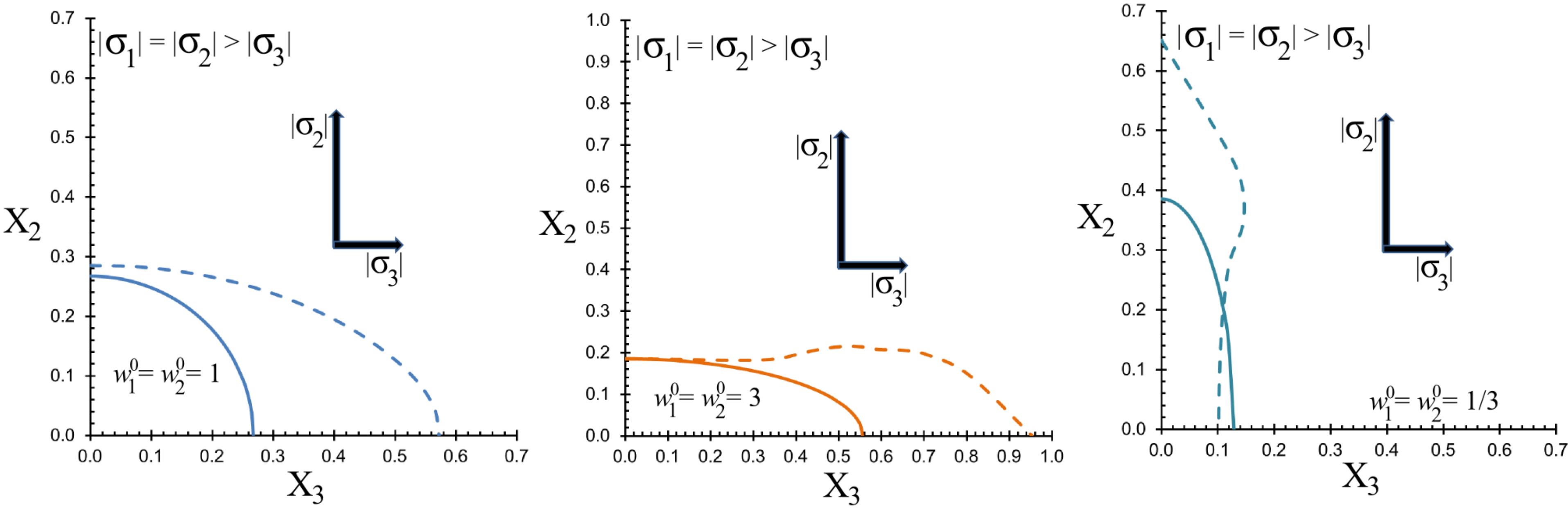

Mbiakop et al., EJMSOL/A, 2015

Switch to

Monotonic loadings

Creep tests in single crystals

Nearly spherical pores

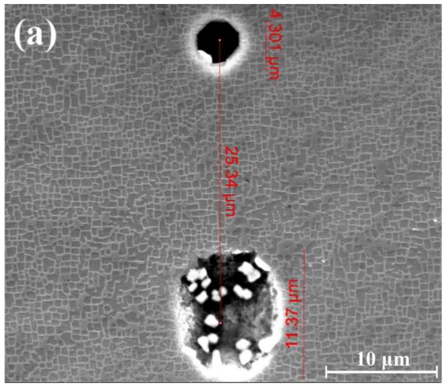

Irregular void shapes

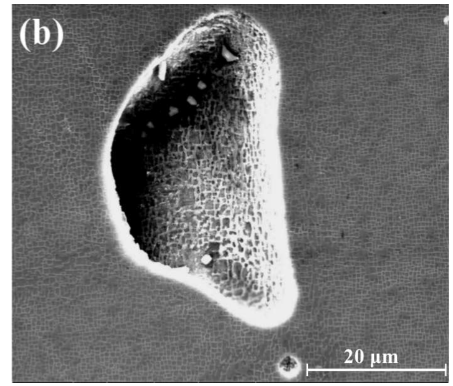

- h=51.8mm specimen

After 51h

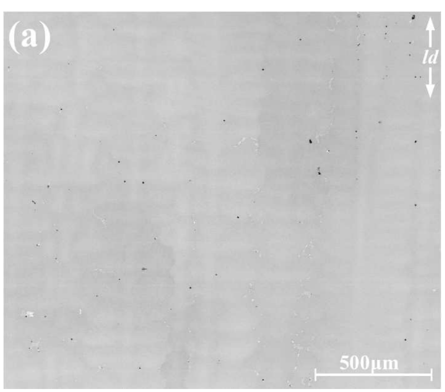

At rupture

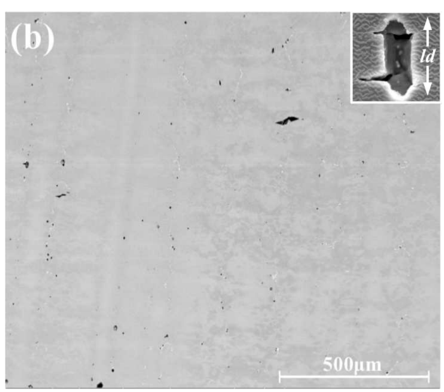

- h=3.18mm specimen

After 78h

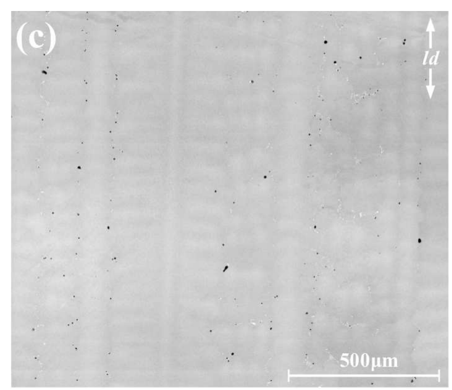

At rupture

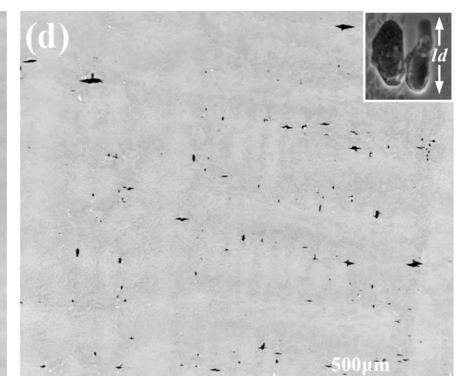

[Shrivastava, Thesis, 2013]

Dual Phase Thin Sheets

1) Large Thin sheets, Active zone 4mm, Grain size ~20µm

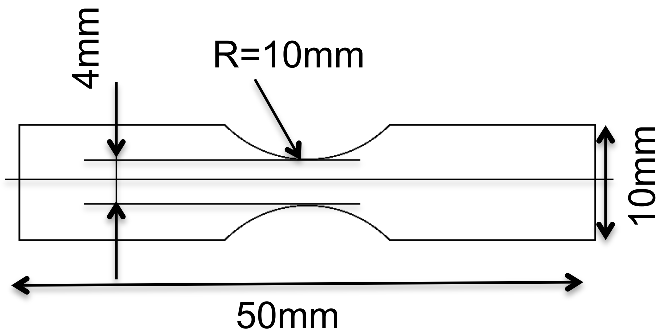

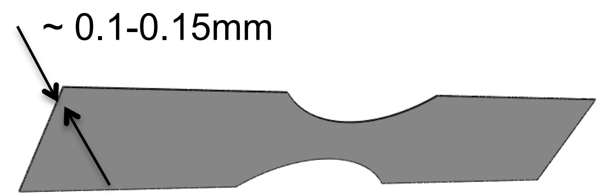

2) Small Thin sheets, Active zone 200µm, Grain size ~20µm

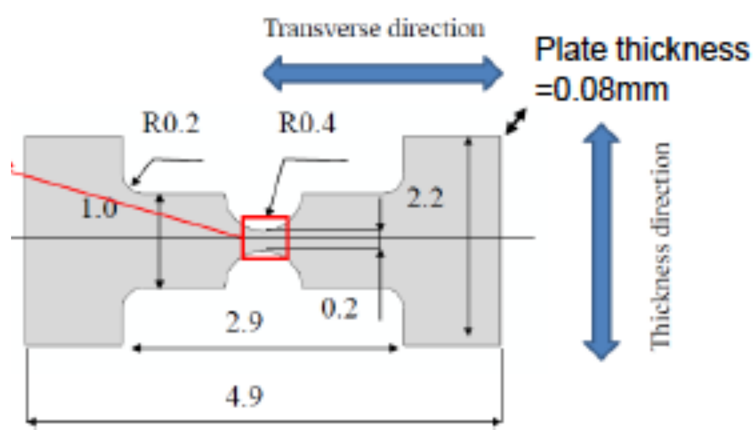

NIPPON STEEL & SUMITOMO METAL CORPORATION

Dual Phase Thin sheets inside SEM

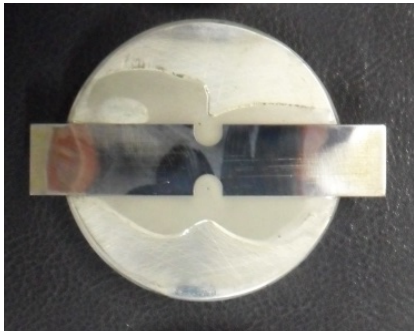

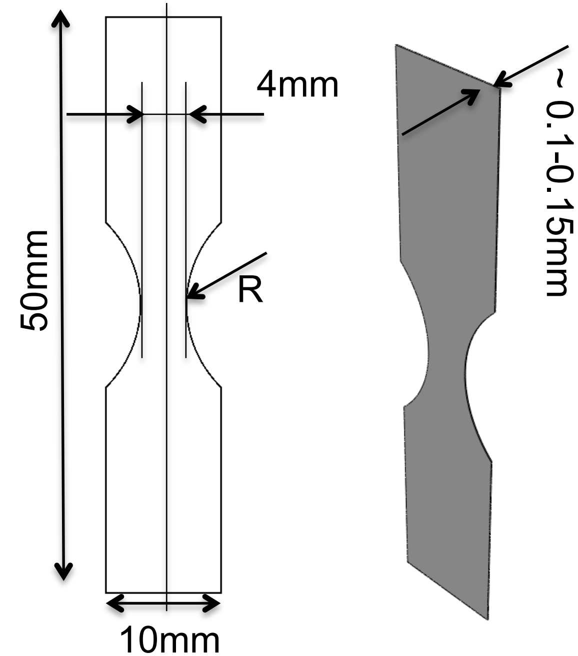

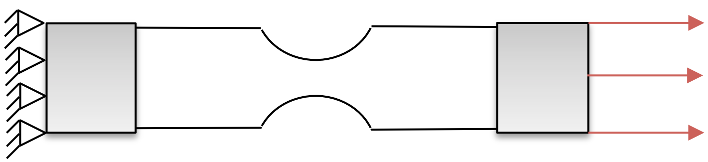

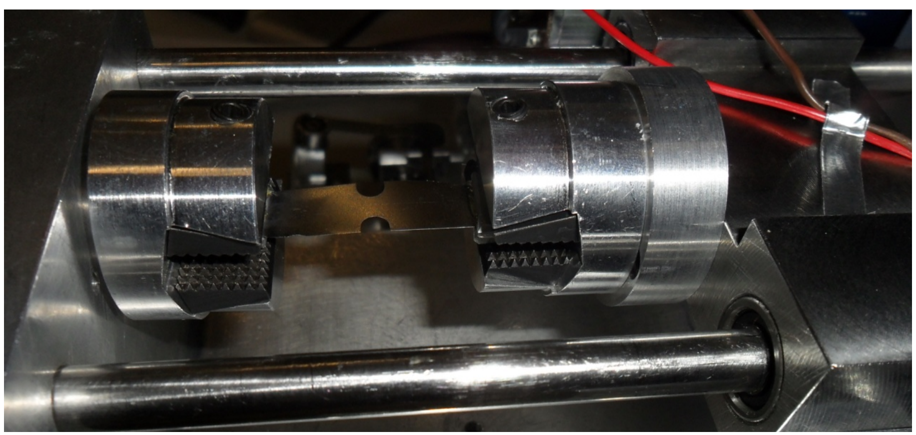

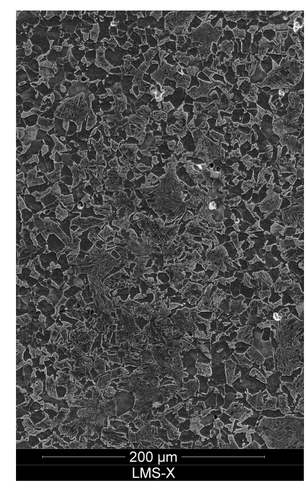

Joint work with Eva Heripre, LMS, SEM

In situ SEM Dual Phase experiments

Joint work with Eva Heripre, LMS, SEM

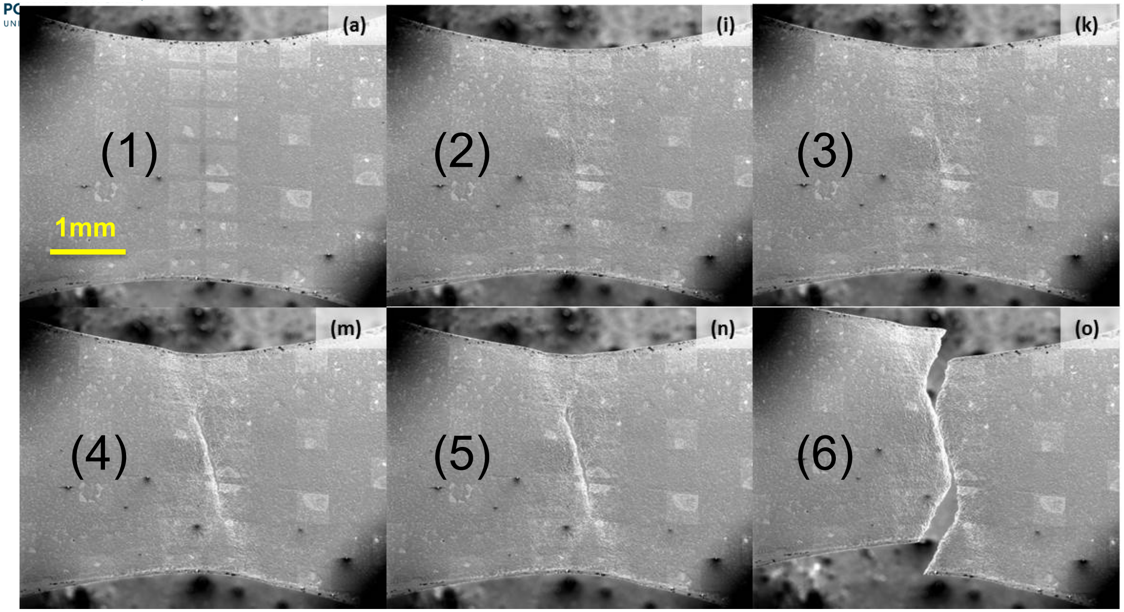

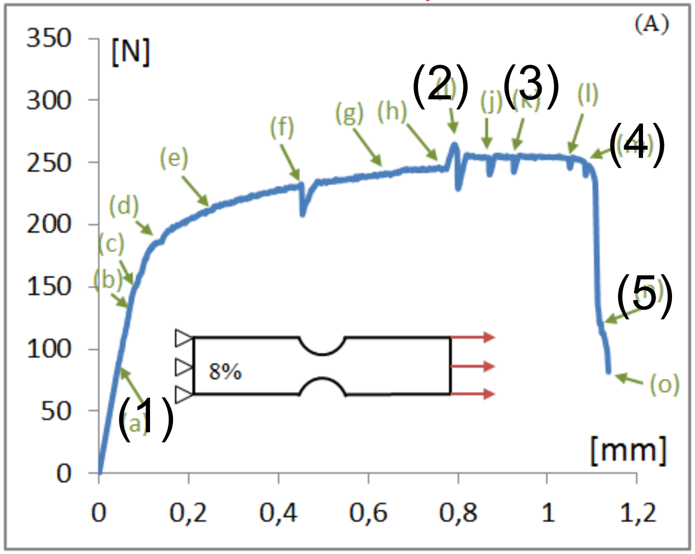

$\varepsilon_{11}+\varepsilon_{22}$

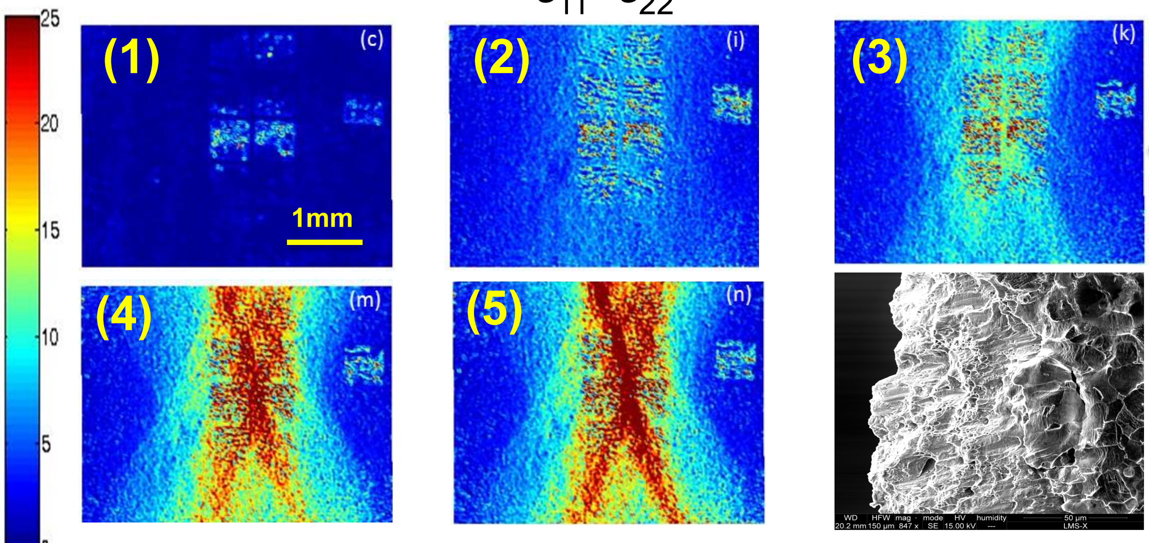

$\varepsilon_{11}+\varepsilon_{22}$

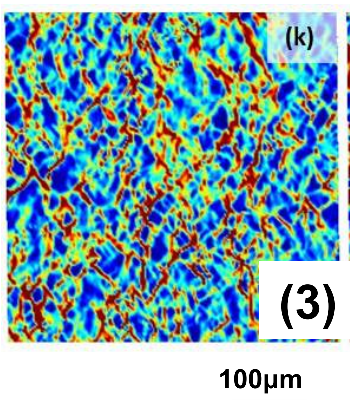

Dual Phase Thin sheets : Small specimens

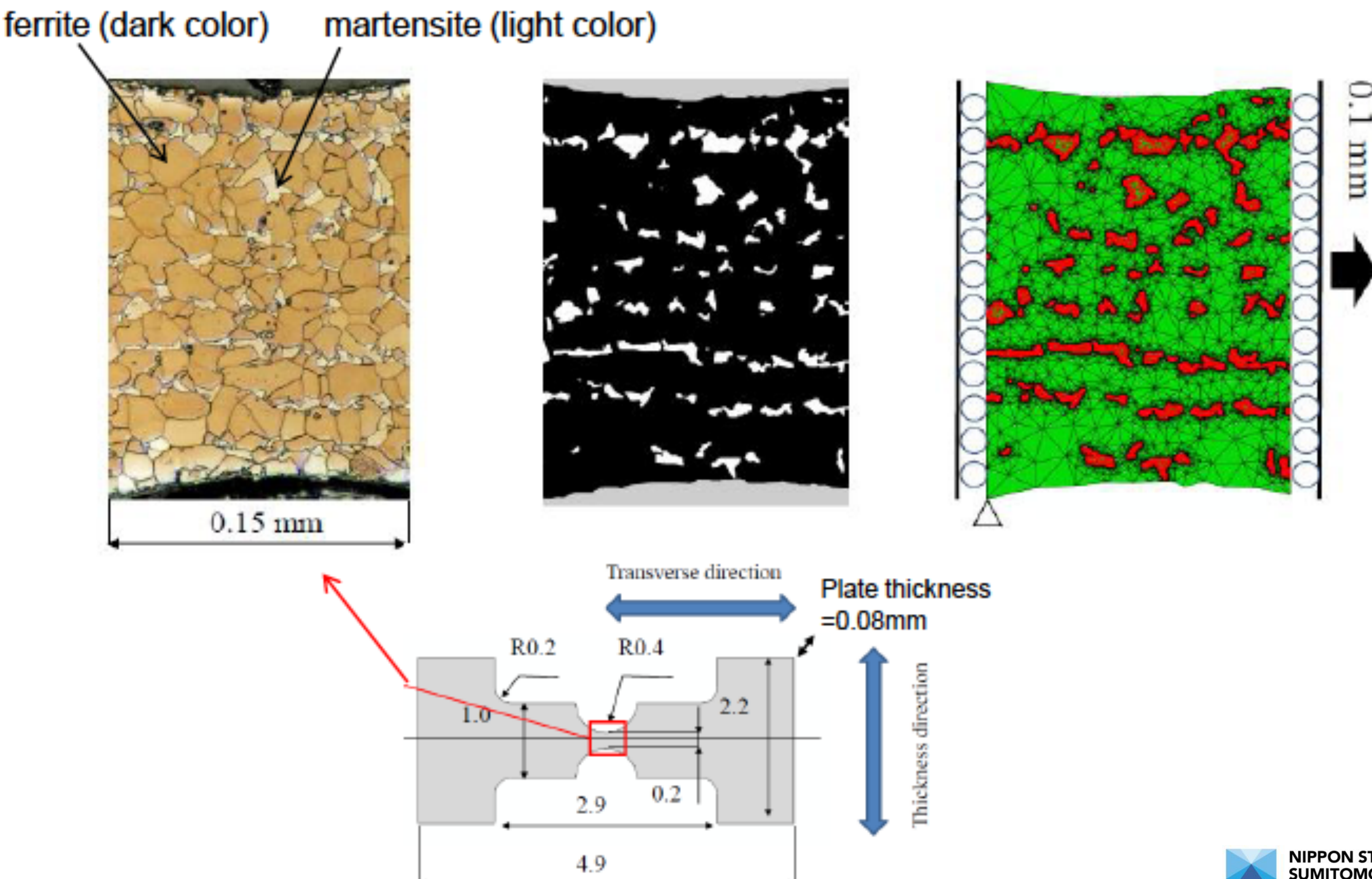

NIPPON STEEL & SUMITOMO METAL CORPORATION

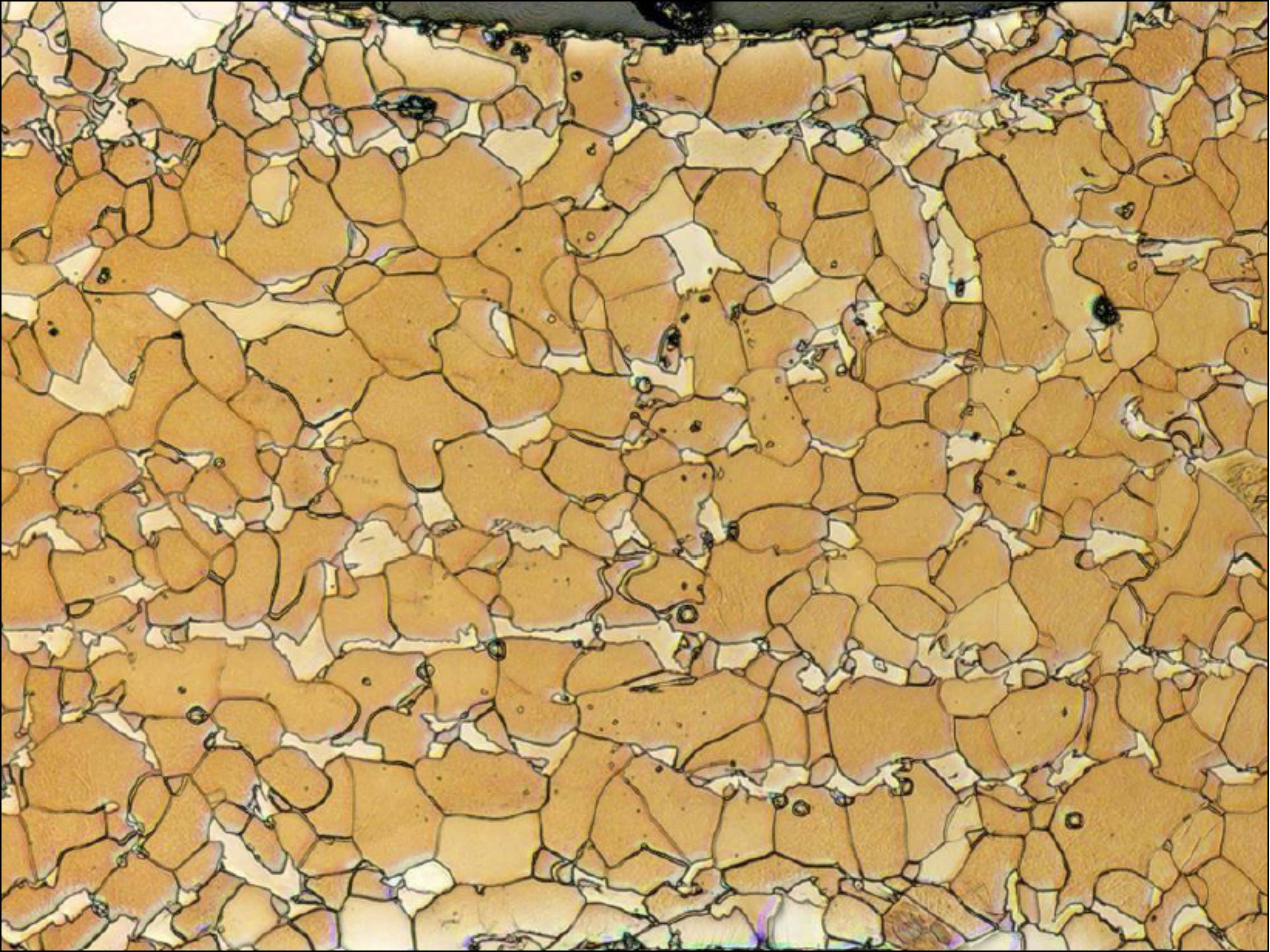

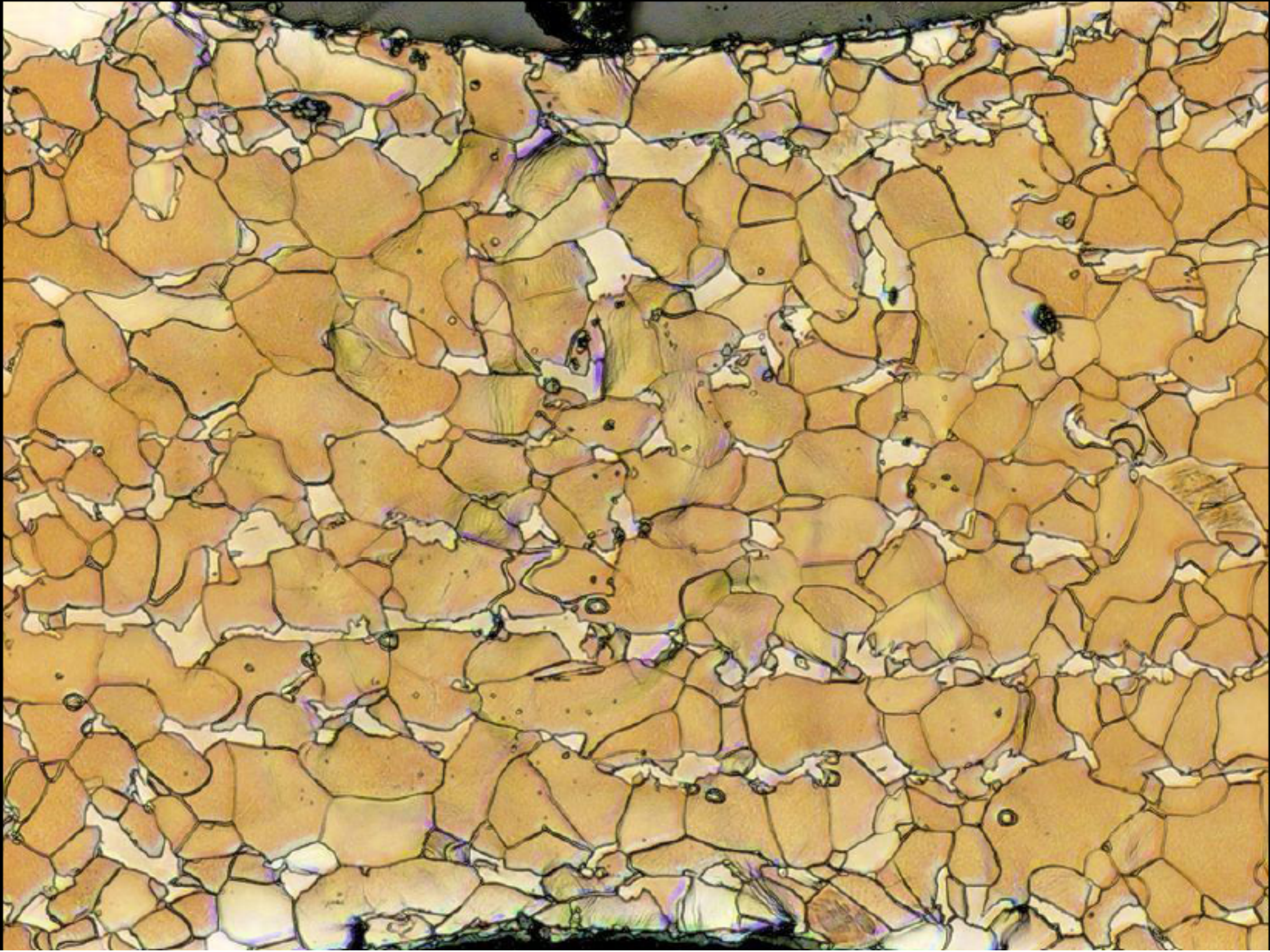

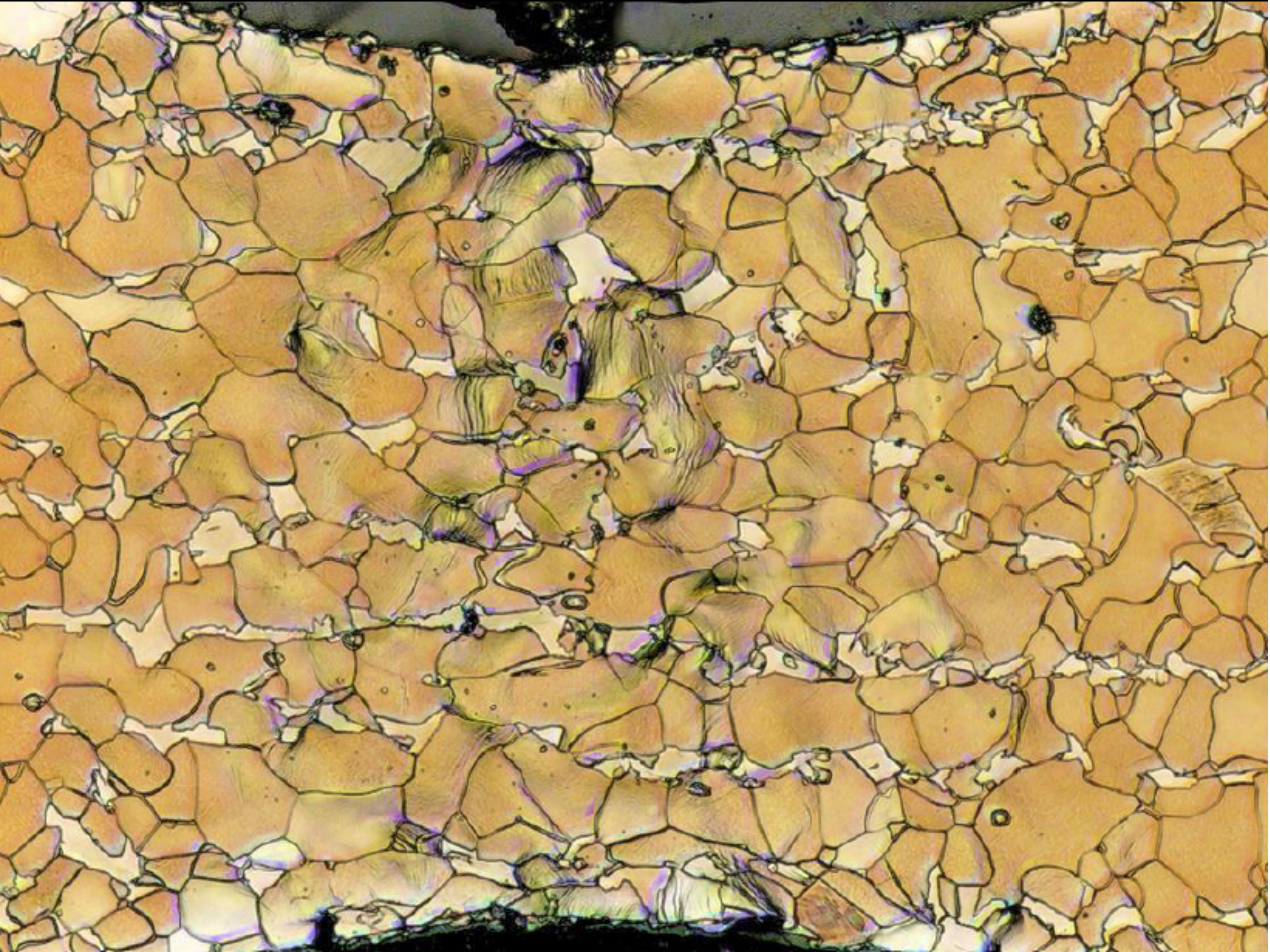

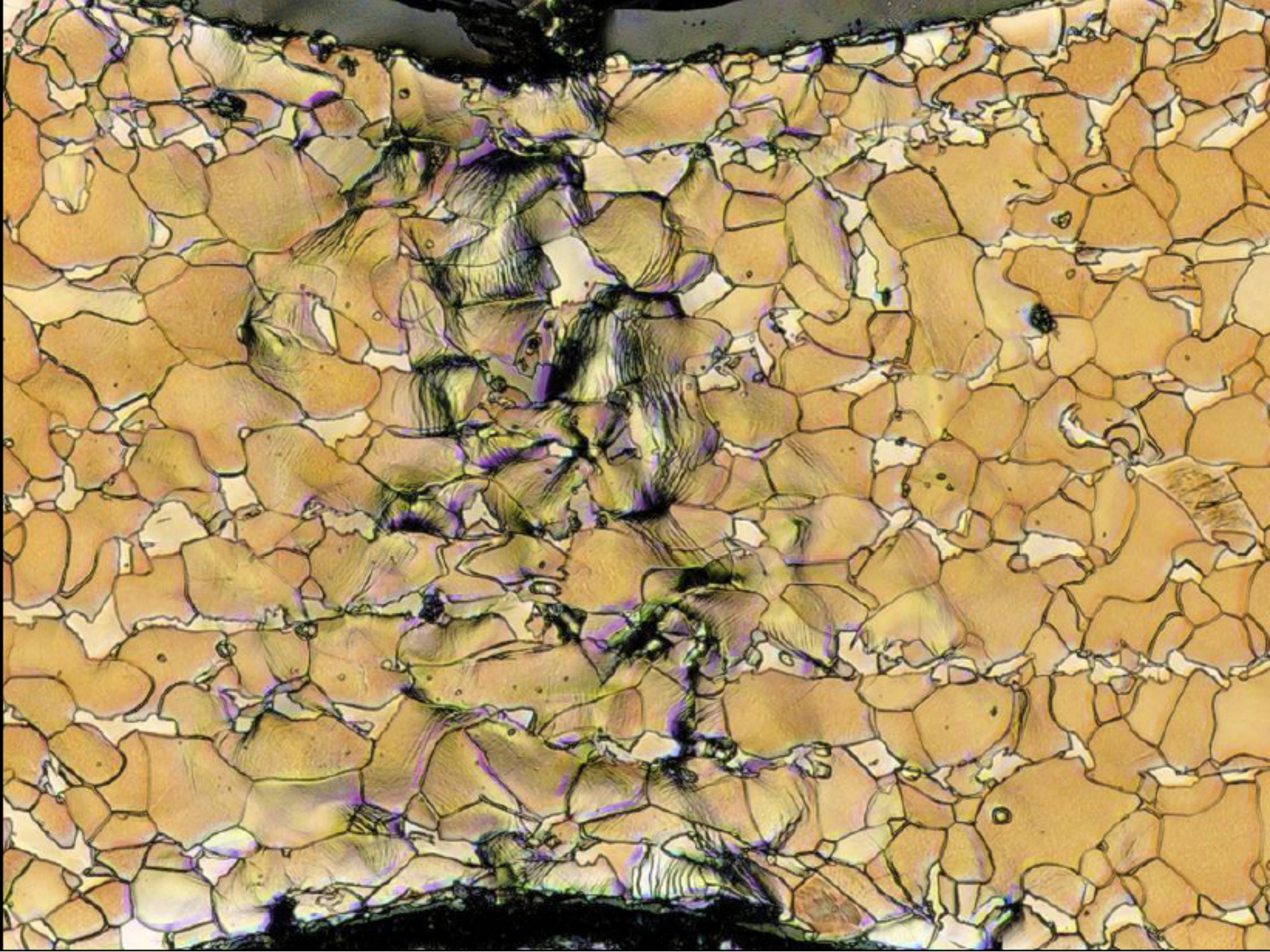

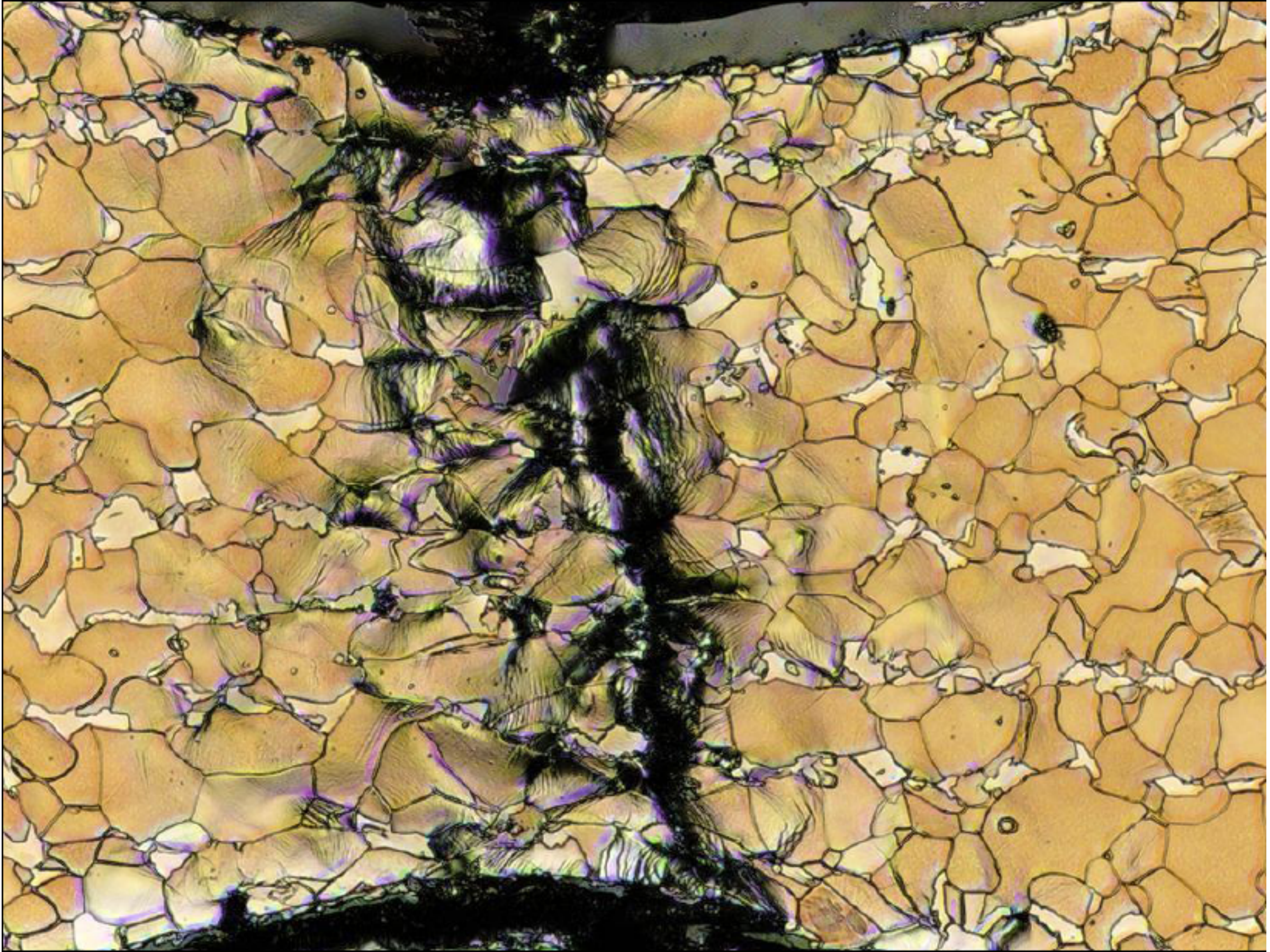

Material & Structural failure

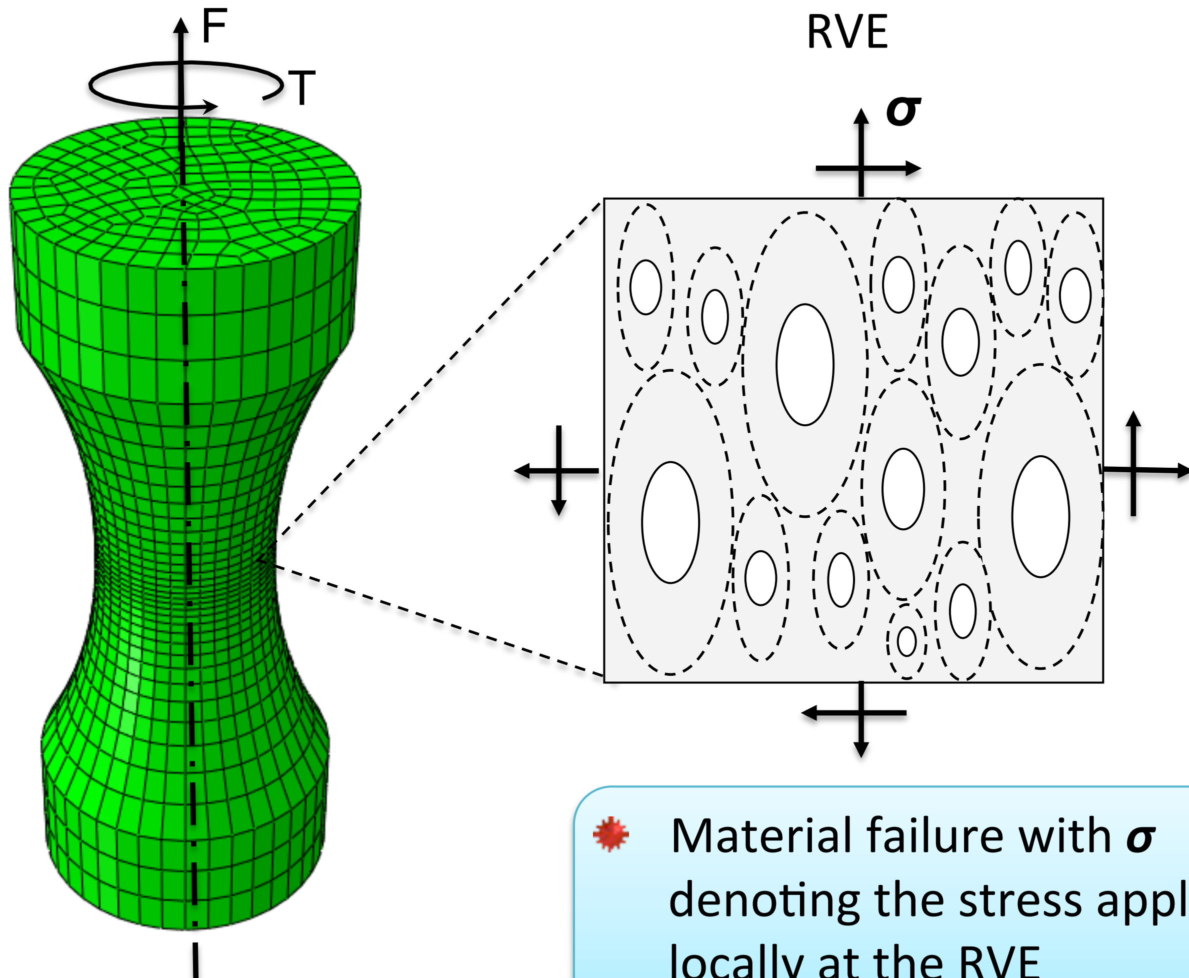

- Material failure with $\boldsymbol{\sigma}$ denoting the stress applied locally at the RVE

- Structural failure with F, T denoting the macroscopic loading conditions

Linear Comparison Composite (LCC)

&

Structure of equations in a nutshell

The LCC homogenization methods

- <u>Instantaneous response</u>
  - Variational (VAR) or Secant method
    Ponte Castañeda (1991)
    Suquet (1993)
  - Second-Order (SOM) or "genaralized secant" method
    Ponte Castañeda (2002)

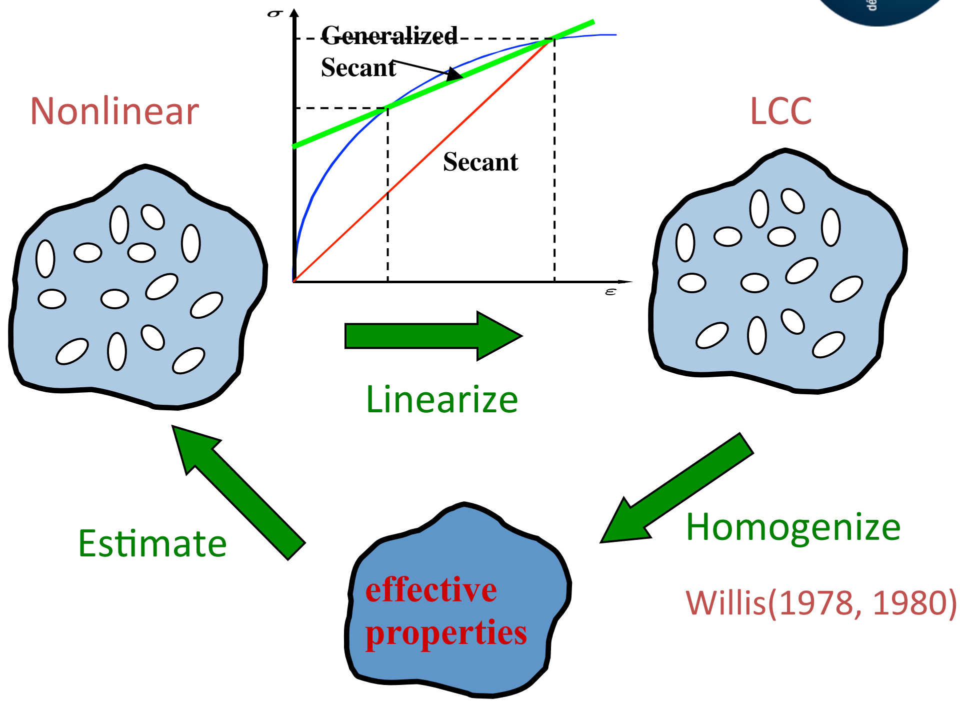

- <u>Evolution of microstructure</u>
  - Void growth
  - Void shape effects
  - Rotation of voids

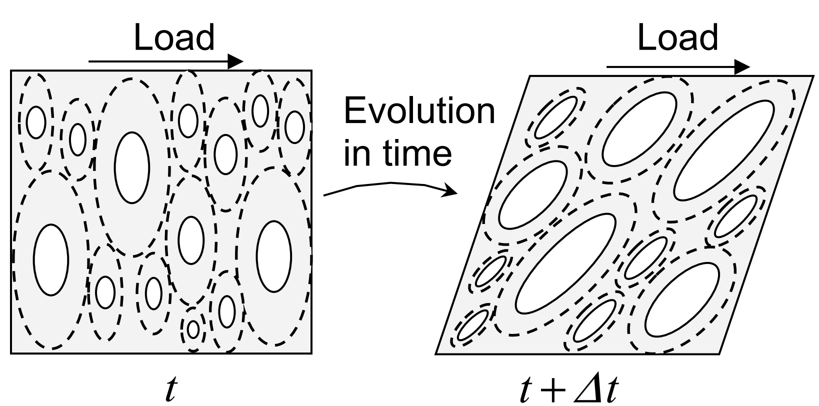

Kailasam & PC, JMPS, (1998), Danas & PC, Eur. J. Mech A (2009), Danas & Aravas, Comp. Part B (2012)

The variational problem

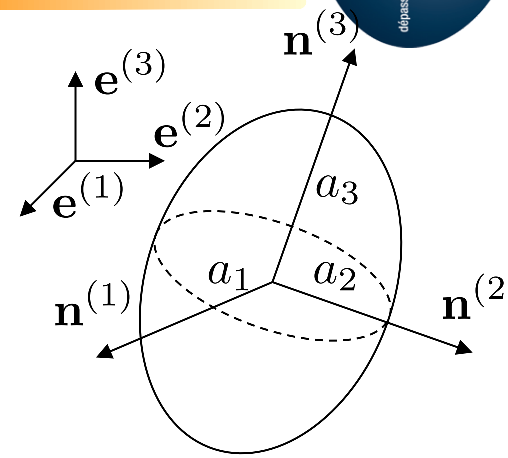

- The original variational form

$$\widetilde{U}(\overline{\boldsymbol{\sigma}}) = (1-f) \min_{\sigma \,\epsilon\, \mathcal{S}(\overline{\sigma})} \int_{V_m} U(\boldsymbol{\sigma}, \mathbf{x}) \mathrm{d}V$$

  - Requires choice of divergence free stress fields
  - Equivalent formulation in strains requires compatible strain fields

- The modified variational principle (Ponte Castaneda, JMPS, 1991)

$$\widetilde{U}_{VAR}(\overline{\boldsymbol{\sigma}}) = \sup_{\mathbf{M}} \left\{ \widetilde{U}_L(\overline{\boldsymbol{\sigma}}; \mathbf{M}) + (1-f) \min_{\hat{\sigma}} \left[U(\hat{\boldsymbol{\sigma}}) - U_L(\hat{\boldsymbol{\sigma}}, \mathbf{M}) \right] \right\}$$

$\mathbf{M}$: Is the elastic compliance of the LCC

  - The “min” operation is relaxed
  - The **M** is chosen so that simple estimates are derived

Structure of evolution problem

- Kinematics: $\dot{\boldsymbol{\varepsilon}} = \dot{\boldsymbol{\varepsilon}}^e + \dot{\boldsymbol{\varepsilon}}^p$
- Elasticity:

$$\dot{\boldsymbol{\sigma}} = \mathbf{L}\,\dot{\boldsymbol{\varepsilon}}, \quad \mathbf{L} = \mathbf{L}^{HS}(f, \mathbf{P}(w_1, w_2, \mathbf{n}^{(i)}))$$

Eshelby-Hill tensors

- Yield condition:

$$\boxed{\Phi(\boldsymbol{\sigma}) = \widehat{\sigma}_e(\boldsymbol{\sigma}; f, \mathbf{P}(w_1, w_2, \mathbf{n}^{(i)})) - \sigma_y(\varepsilon_M^p) = 0}$$

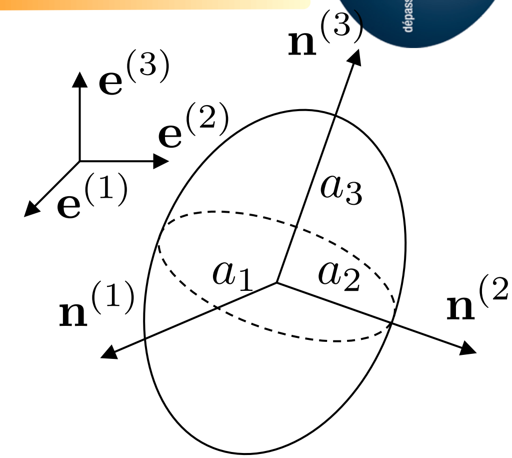

$$w_1 = a_3/a_1$$
$$w_2 = a_3/a_2$$

Evolution of microstructure

- Porosity evolution: $\dot{f} = (1-f)\dot{\varepsilon}_{kk}^p$
- Void shape evolution: $\dot{w}_i = \alpha_w\, w_i \left(\mathbf{n}^{(3)}\mathbf{n}^{(3)} - \mathbf{n}^{(i)}\mathbf{n}^{(i)}\right) : \dot{\boldsymbol{\varepsilon}}^v, \;\; i = 1, 2$
- Void orientation evolution: $\dot{\mathbf{n}}^{(i)} = \boldsymbol{\omega}(\boldsymbol{\Omega}, \dot{\boldsymbol{\varepsilon}}^v) \cdot \mathbf{n}^{(i)}$

Crystal Plasticity Yield functions

Modified VAR (MVAR)

(Mbiakop, Constantinescu, Danas, IJSS, in press)

The constitutive response of the matrix

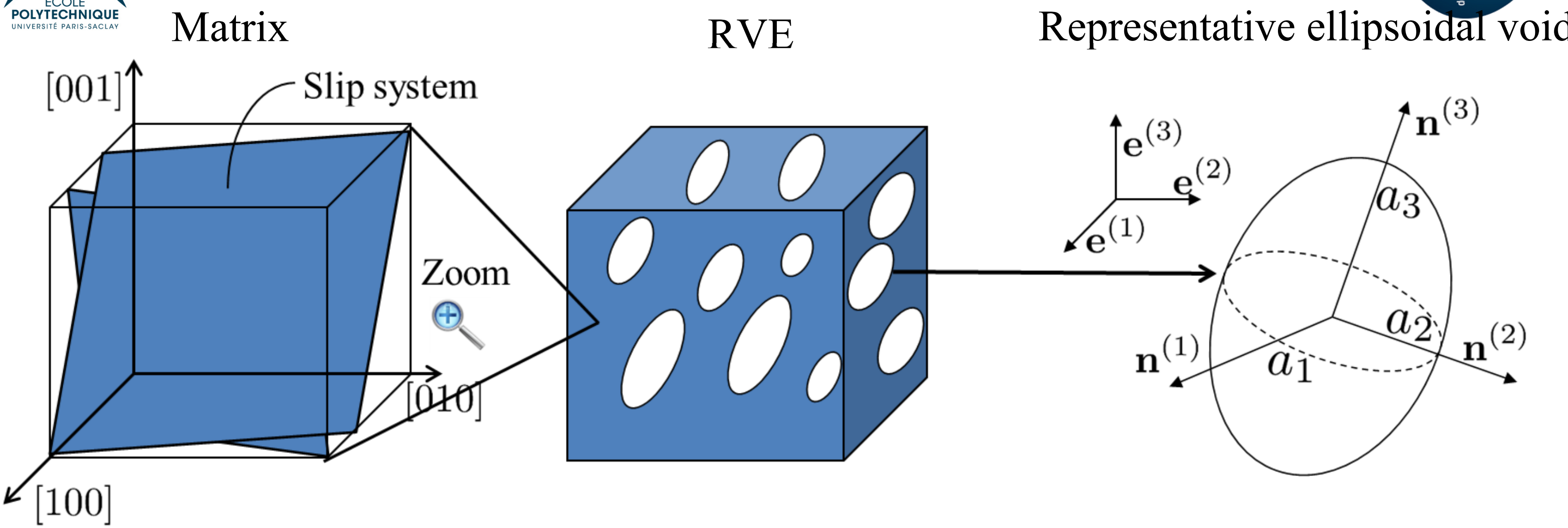

$$U(\boldsymbol{\sigma}) = \sum_{s=1}^{K} \Psi^{(s)}(\tau^{(s)}) = \sum_{s=1}^{K} \frac{\dot{\gamma}_0^{(s)} \tau_0^{(s)}}{n+1} \left(\frac{\left|\tau^{(s)}\right|}{\tau_0^{(s)}} \right)^{n+1}$$

- Schmid tensor : $\boldsymbol{\mu}^{(s)} = \frac{1}{2} \left(\mathbf{m}^{(s)} \otimes \mathbf{s}^{(s)} + \mathbf{s}^{(s)} \otimes \mathbf{m}^{(s)} \right)$
- CRSS stress & slip: $\tau^{(s)} = \boldsymbol{\sigma} \cdot \boldsymbol{\mu}^{(s)}$ $\qquad \gamma^{(s)} = \frac{\partial \Psi^{(s)}}{\partial \tau^{(s)}}(\tau^{(s)})$

The MVAR yield function

- For a J2-plastic matrix (PC, 1991)

$$\widetilde{\Phi}_{mvar}(\overline{\boldsymbol{\sigma}}) = \max_{s=1,K}\left\{\sqrt{\frac{\overline{\boldsymbol{\sigma}}\cdot\mathbf{m}^{(s)}\cdot\overline{\boldsymbol{\sigma}}}{1-f}} - (\tau_0)^{(s)}\right\} = 0$$

$$\mathbf{m}^{var,(s)} = \boldsymbol{\mu}^{(s)}\otimes\boldsymbol{\mu}^{(s)} + \frac{f}{K}\left(\mathbf{Q}^{-1} - \sum_{s=1}^{K}\boldsymbol{\mu}^{(s)}\otimes\boldsymbol{\mu}^{(s)}\right), \quad \mathbf{Q} = g(\mathbf{P},\boldsymbol{\mu},\boldsymbol{\mathcal{J}})$$

- A simple correction on the hydrostatic part only

$$\mathbf{m}^{(s)} = \mathbf{m}^{var,(s)} + \left(q_J^2 - 1\right)\boldsymbol{\mathcal{J}}\cdot\mathbf{m}^{var,(s)}\cdot\boldsymbol{\mathcal{J}}$$

$$q_J = \sqrt{\frac{5}{2}}\frac{1-f}{\sqrt{f}\,\ln(1/f)}$$

Mbiakop Constantinescu and Danas, IJSS, in press 2D; and in preparation 3D

BCC with spherical voids

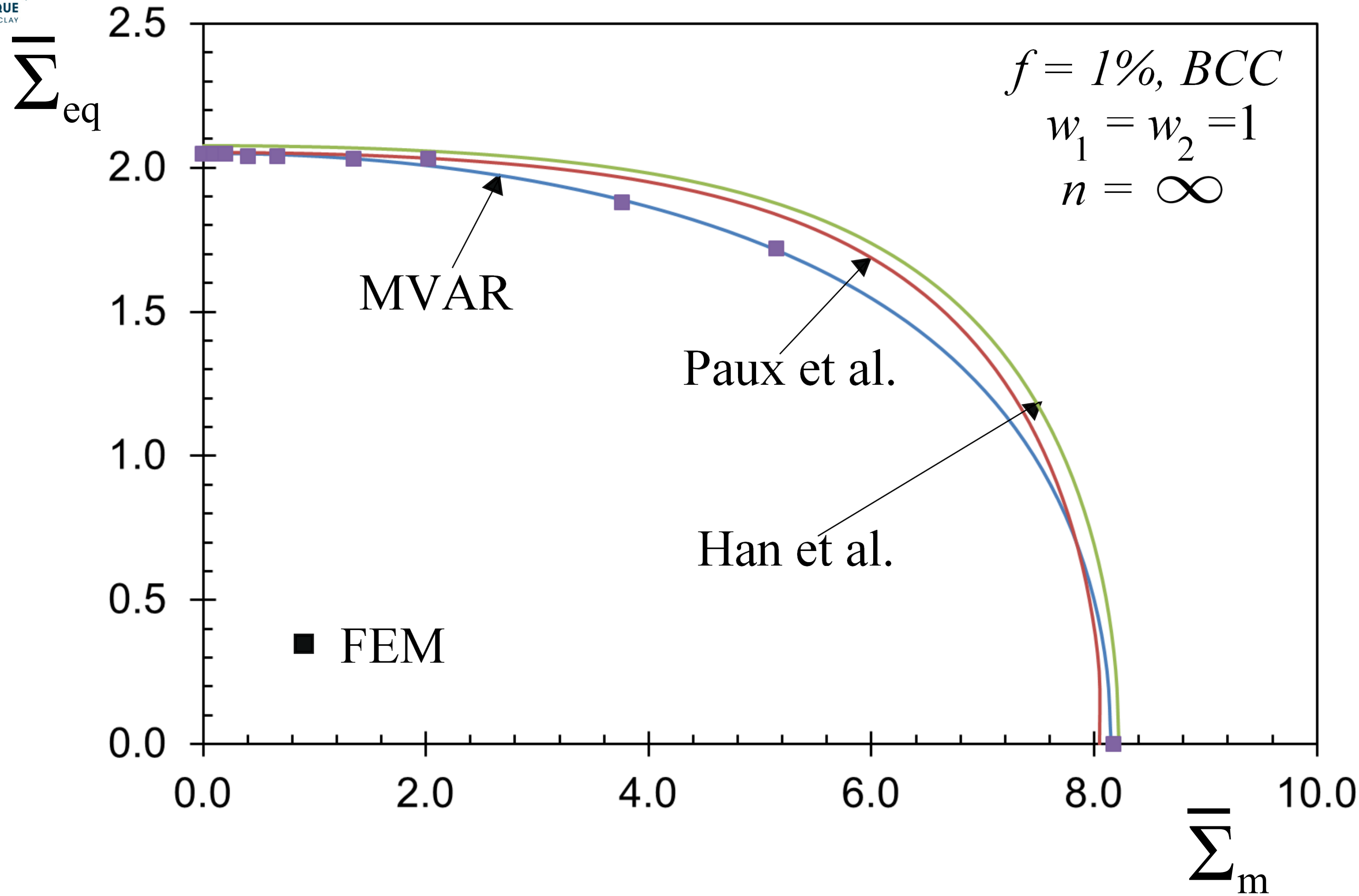

- All models show the same features and minor differences are observed

Han et al, IJSS, 2013; Paux et al., EJMSOL/A, 2015; Mbiakop et al., in prep.

FCC with spherical voids

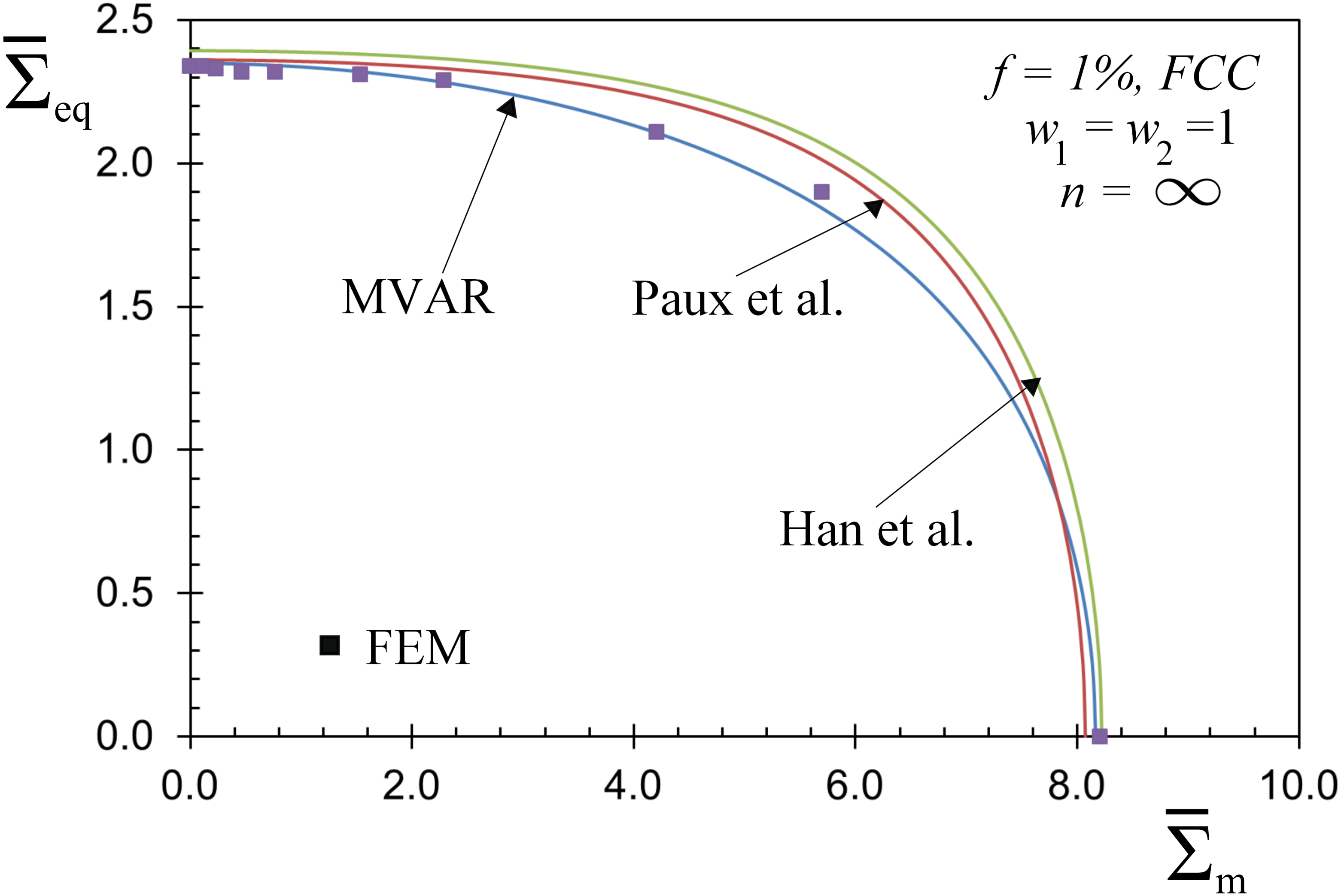

- All models show the same features and minor differences are observed

Han et al, IJSS, 2013; Paux et al., EJMSOL/A, 2015; Mbiakop et al., in prep.

HCP (K=3,6,12) with spherical voids

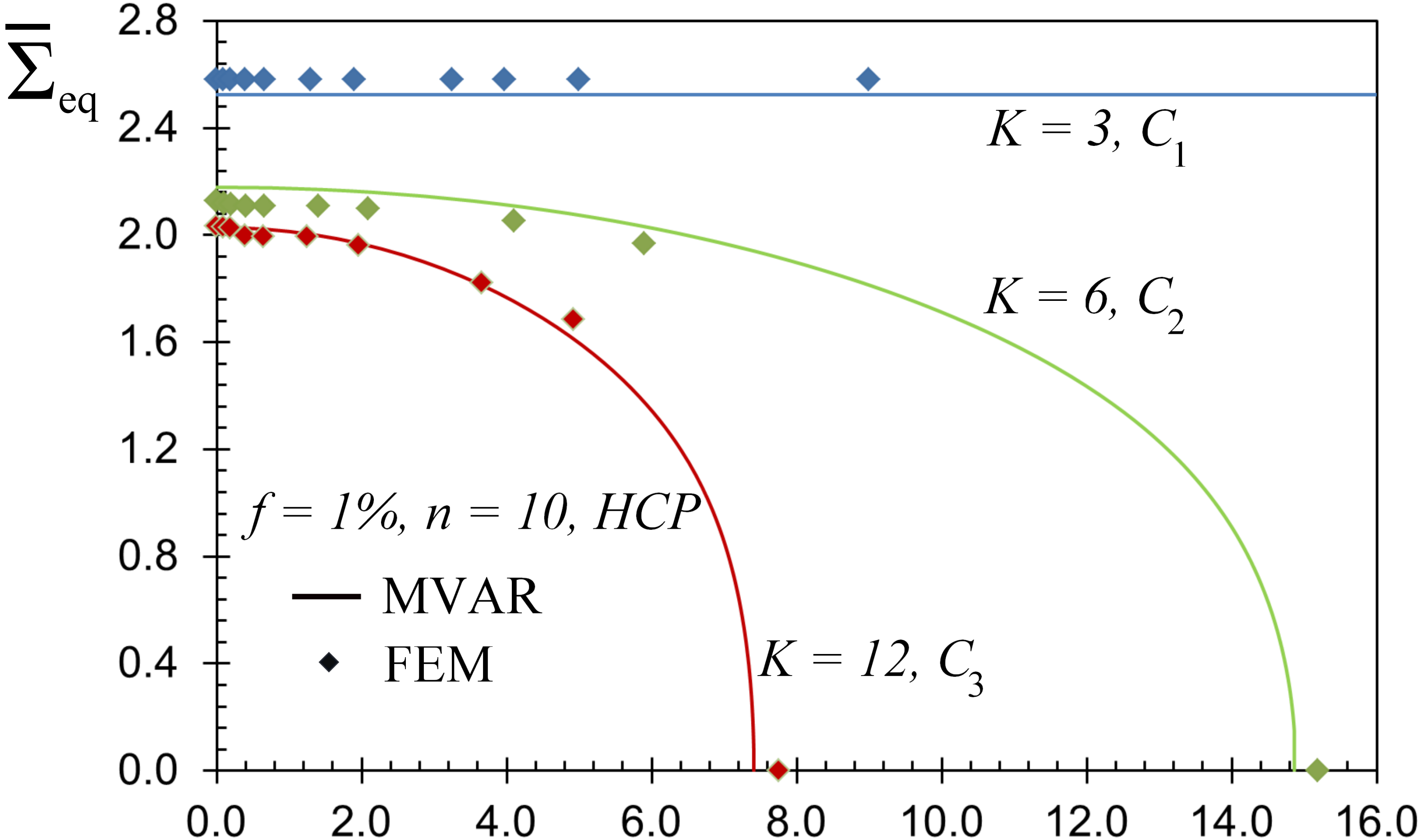

Cases	slip plane $\mathbf{m}$	slip direction $\mathbf{s}$	number of slip systems
C_1	Basal $\{0001\}$	Type $\langle a \rangle$ $\langle 1\bar{2}10 \rangle$	3
C_2	Pyramidal Π_2 $\{11\bar{2}2\}$	Type $\langle c+a \rangle$ $\langle 11\bar{2}3 \rangle$	6
C_3	Pyramidal Π_1 $\{10\bar{1}1\}$	Type $\langle c+a \rangle$ $\langle 11\bar{2}3 \rangle$	12

Han et al, IJSS, 2013; Paux et al., EJMSOL/A, 2015; Mbiakop et al., in prep.

Deviatoric planes for spherical pores

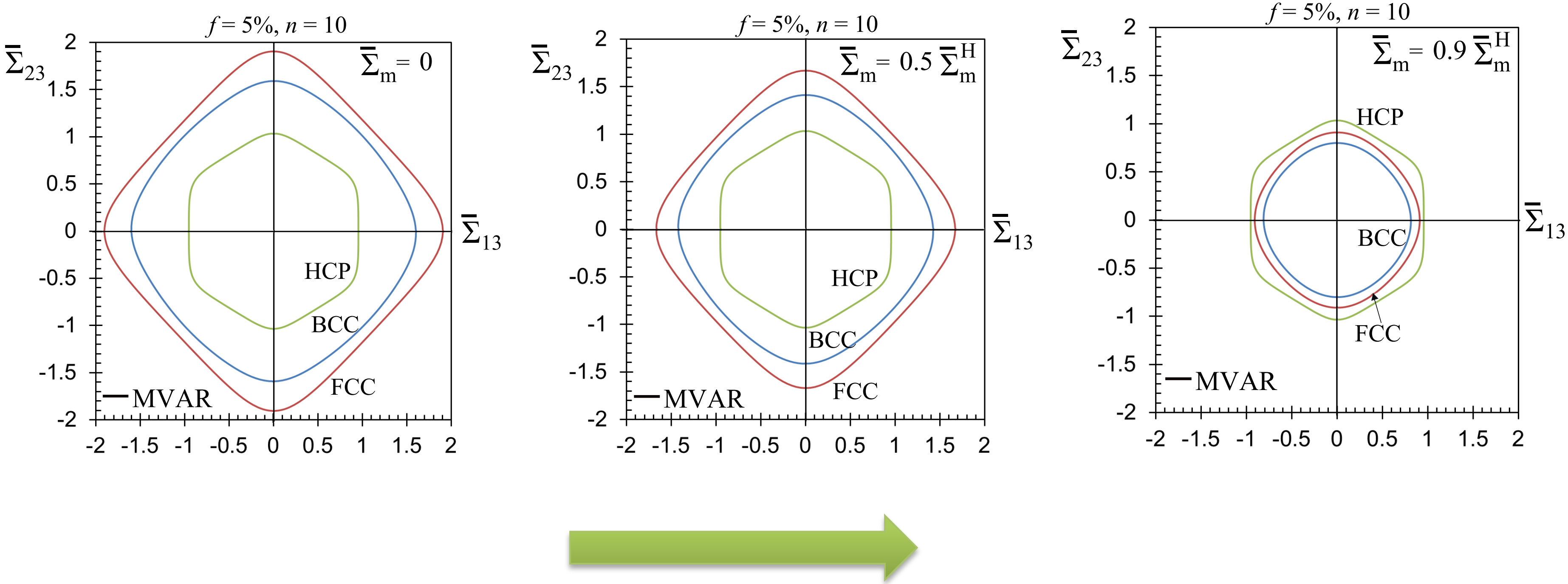

Increasing superposed positive pressure

Effect of void shape in FCC

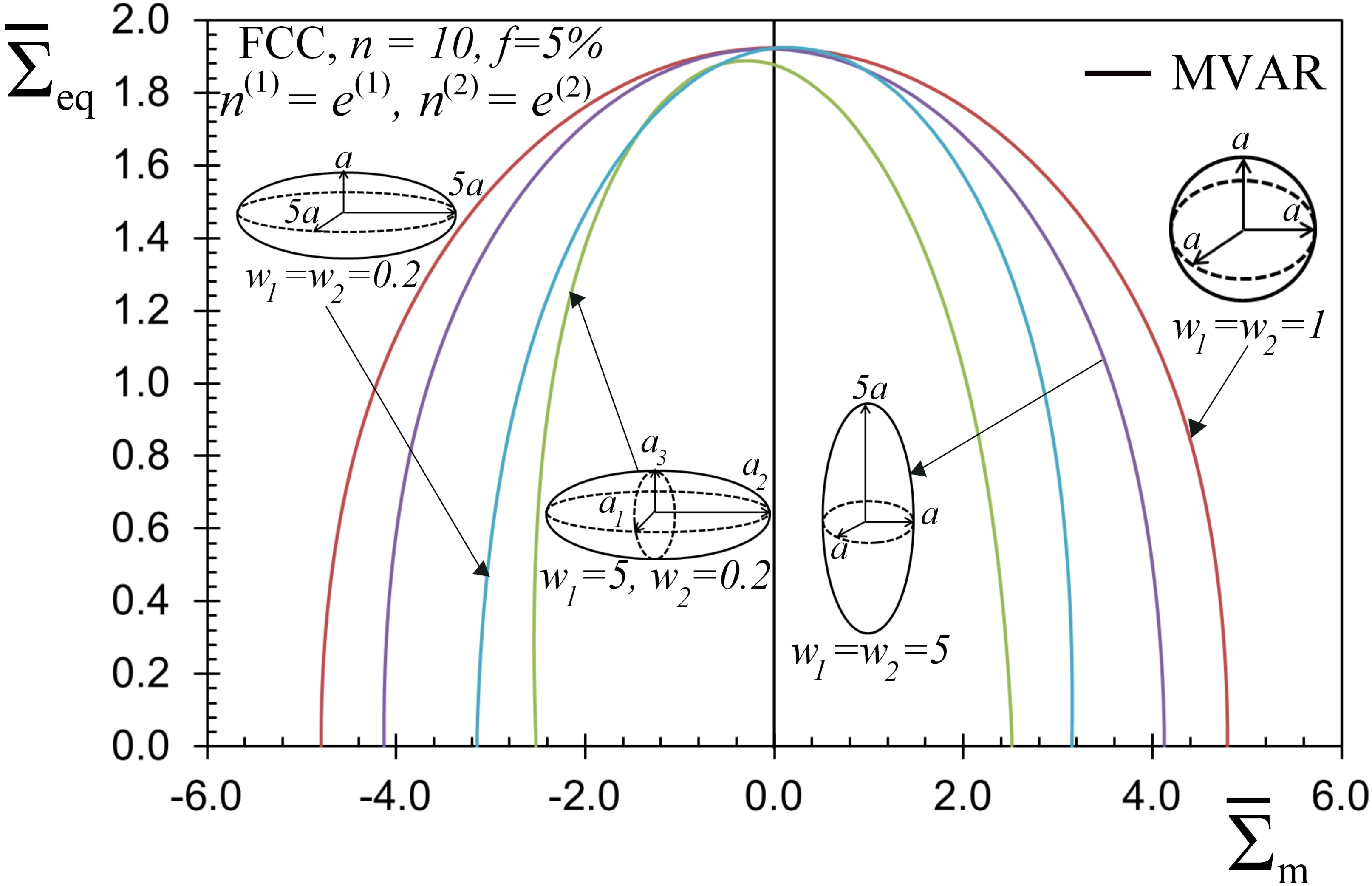

Effect of void shape in FCC : dev plane

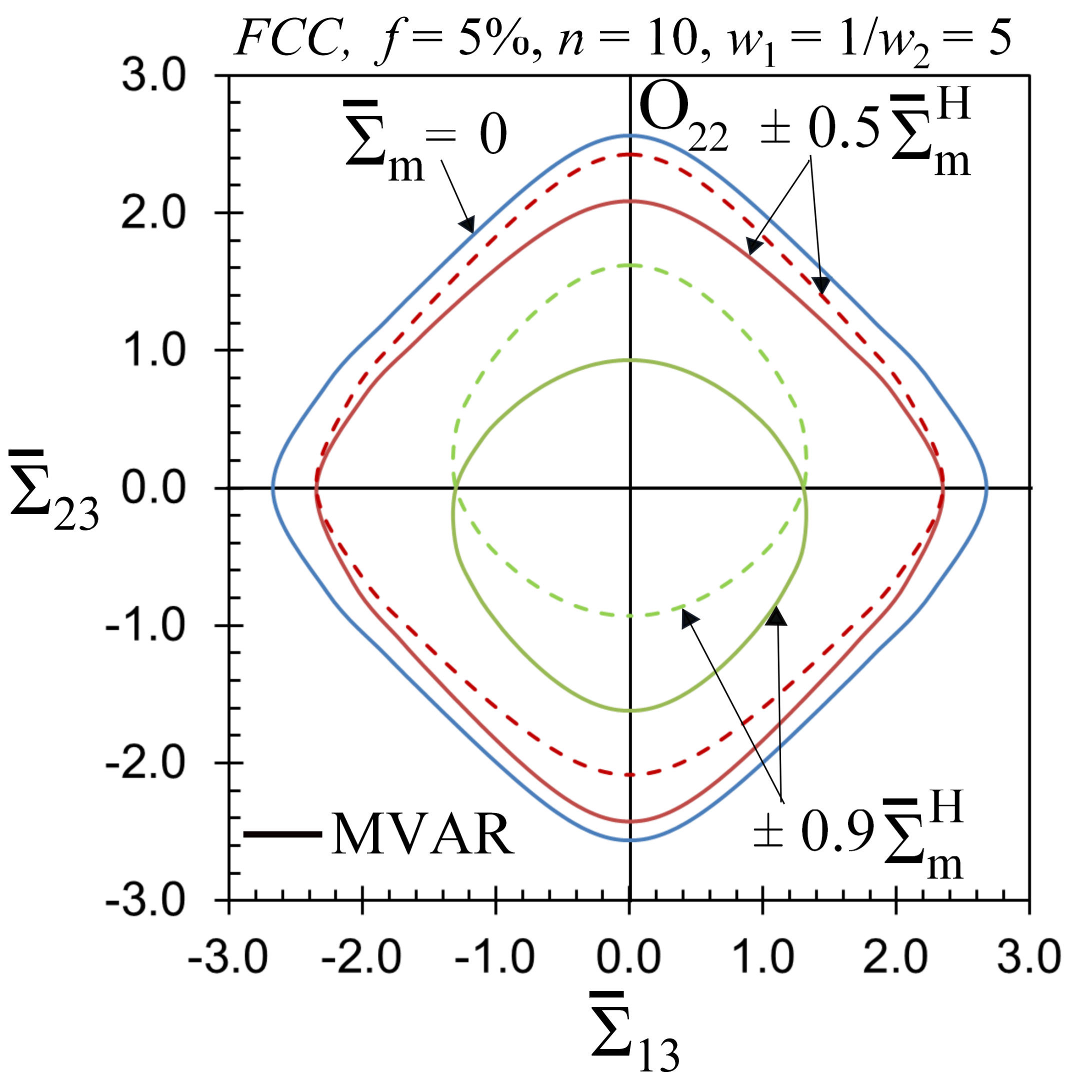

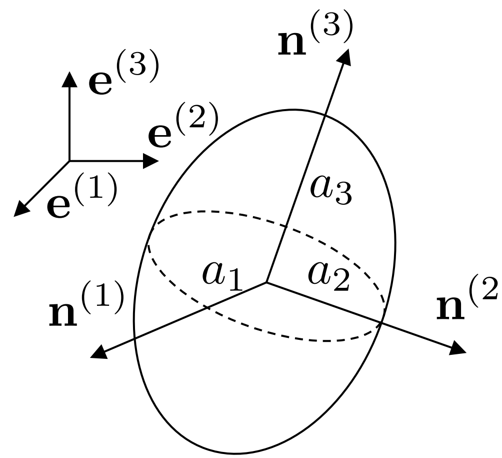

$$w_1 = a_3/a_1$$

$$w_2 = a_3/a_2$$

$$\mathbf{n}^{(1)} = \{1\,0\,1\}$$

$$\mathbf{n}^{(2)} = \{0\,1\,0\}$$

$$\mathbf{n}^{(3)} = \{\bar{1}\,0\,1\}$$

FEM contours : f=1%

Total slip γ_{tot}/γ_0

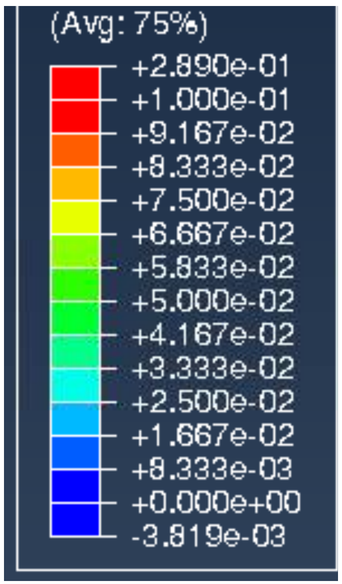

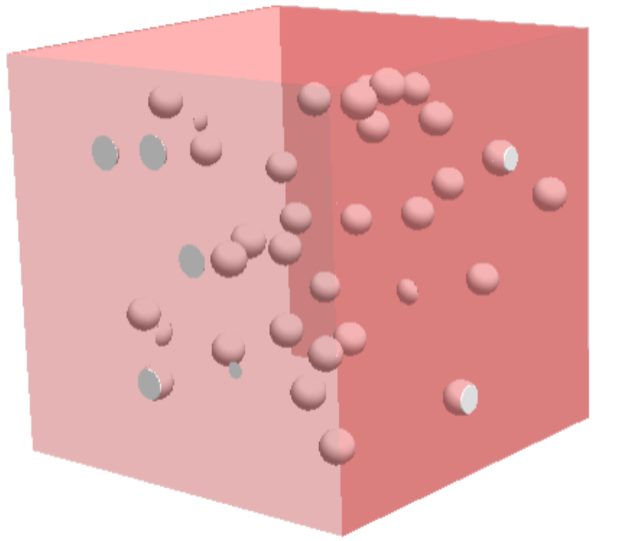

FCC

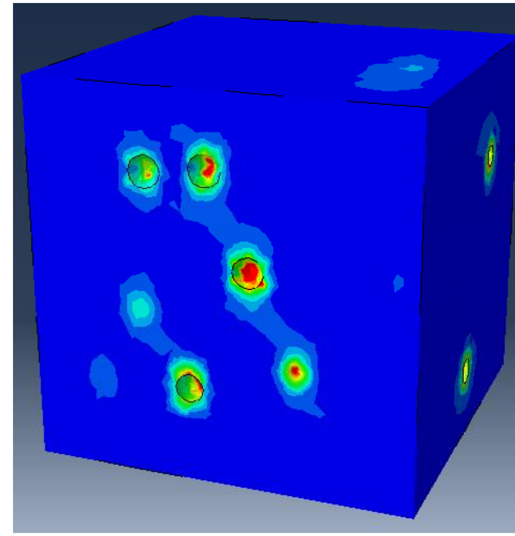

BCC

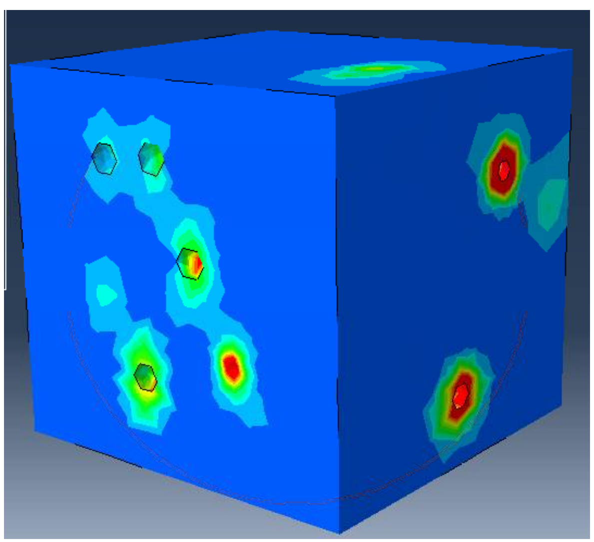

HCP

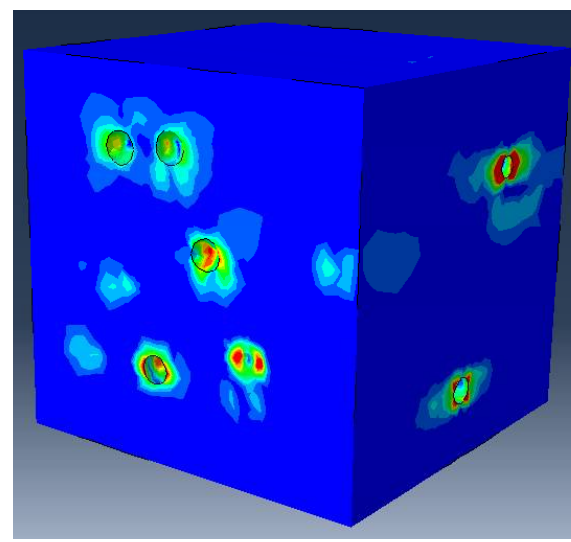

2D cross-sections : FCC crystal

f=1%

f=5%

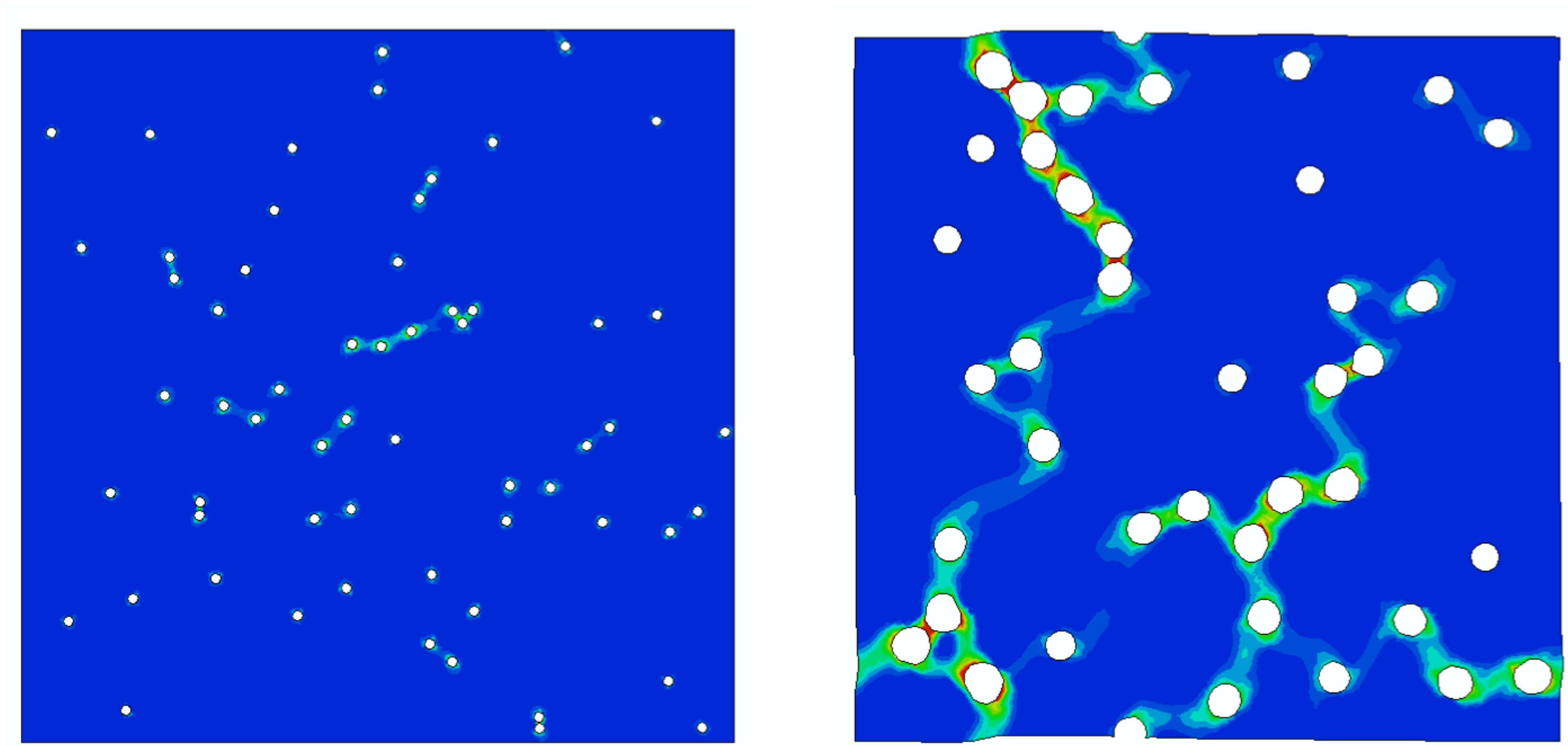

Total slip γ_{tot}/γ_0

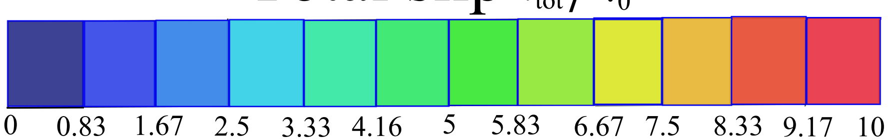

Isotropic MVAR ABAQUS UMAT

Qualitative comparisons with experiments

Danas & Aravas (2012), Composites Part B

But see also

(Son, Maziere, Danas, Besson, IJSS, soon in press)

(GVAR)

The MVAR yield function

- For a J2-plastic matrix (PC, 1991)

$$\Phi(\boldsymbol{\sigma}) = \widehat{\sigma}_e - \sigma_y(\varepsilon_M^p) = 0, \quad \widehat{\sigma}_e = \sqrt{\frac{\sigma_{ij}\, m_{ijkl}\, \sigma_{kl}}{1-f}}$$

$$\mathbf{m}^{var} = \frac{3}{2}\boldsymbol{\mathcal{K}} + \frac{3\,f}{1-f}\mathbf{Q}^{-1}, \quad \mathbf{Q} = g(\mathbf{P}, \boldsymbol{\mathcal{K}}, \boldsymbol{\mathcal{J}})$$

- A simple correction on the hydrostatic part only

(PC, 1992; Michel & Suquet, 1992)

$$\mathbf{m}^{mvar} = \mathbf{m}^{var} + (q_J^2 - 1)\,\boldsymbol{\mathcal{J}} \cdot \mathbf{m}^{var} \cdot \boldsymbol{\mathcal{J}}, \qquad q_J = \frac{1-f}{\sqrt{f}\,\ln(1/f)}$$

- MVAR : Recovers the optimal bound for hydrostatic loadings & spherical or cylindrical (non-trivial) voids
- The predictions for arbitrary void shapes are extrapolations of this approximation

Yield Surfaces: Isotropic microstructures

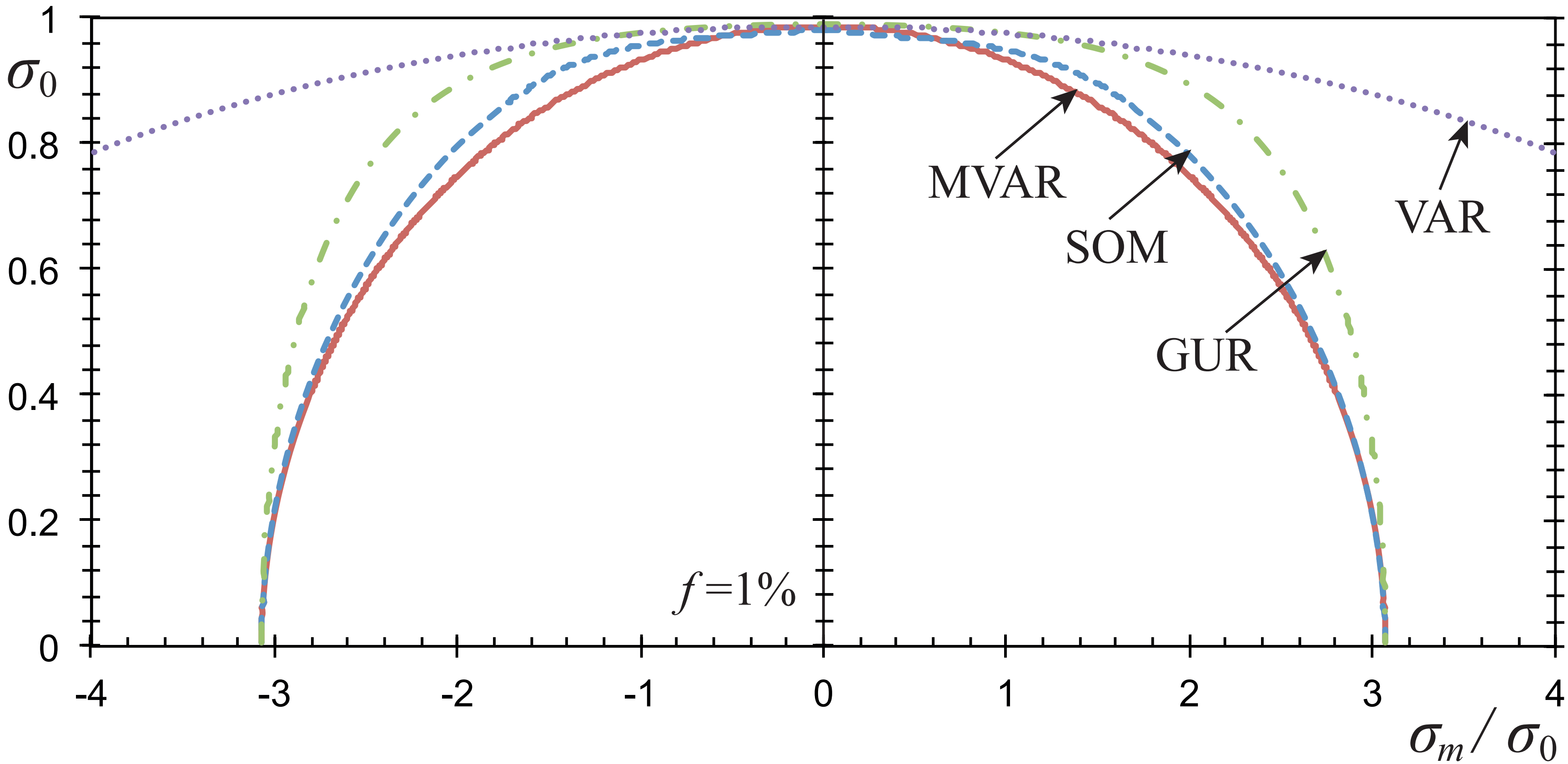

- MVAR is symmetric w.r.t. σ_m and slightly more compliant than SOM

But see bounds of PC, 2013, Agoras and PC, IJSS, 2014

Yield Surfaces: Void shape effects

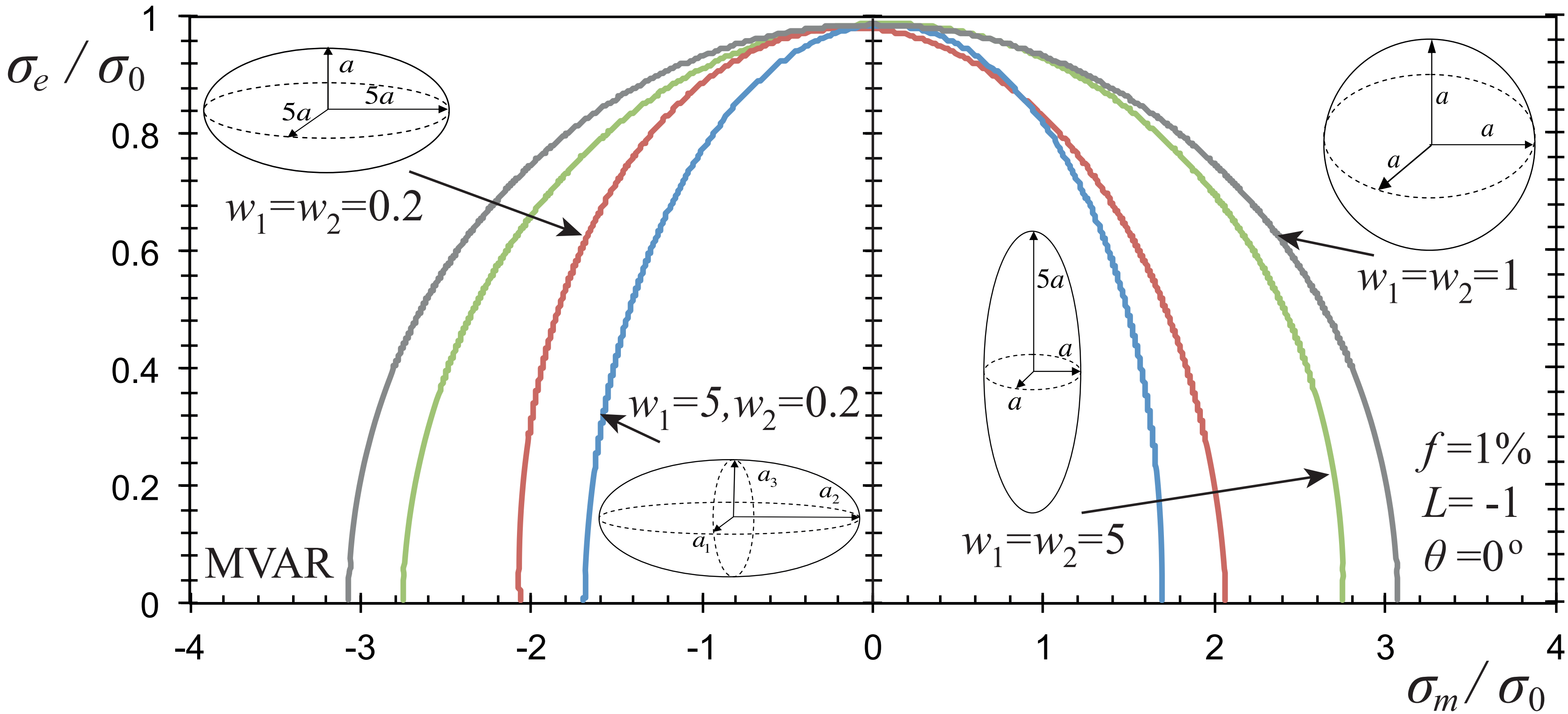

- MVAR is identical to the SOM in the purely hydrostatic limit for any shape

Structure of evolution problem

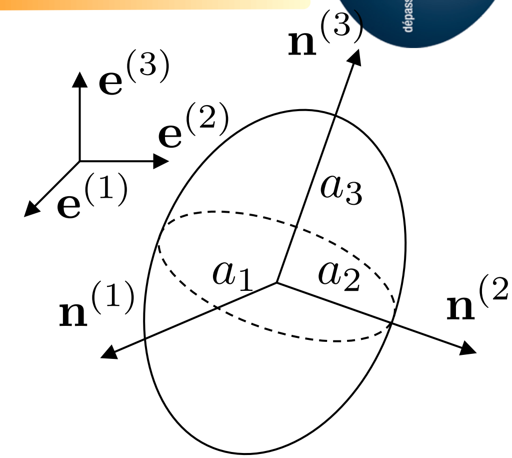

$$w_1 = a_3/a_1$$
$$w_2 = a_3/a_2$$

- Kinematics: $\dot{\boldsymbol{\varepsilon}} = \dot{\boldsymbol{\varepsilon}}^e + \dot{\boldsymbol{\varepsilon}}^p$
- Elasticity:

$$\dot{\boldsymbol{\sigma}} = \mathbf{L}\,\dot{\boldsymbol{\varepsilon}}, \quad \mathbf{L} = \mathbf{L}^{HS}(f, \mathbf{P}(w_1, w_2, \mathbf{n}^{(i)}))$$

Eshelby-Hill tensors

- Yield condition:

$$\boxed{\Phi(\boldsymbol{\sigma}) = \widehat{\sigma}_e(\boldsymbol{\sigma}; f, \mathbf{P}(w_1, w_2, \mathbf{n}^{(i)})) - \sigma_y(\varepsilon_M^p) = 0}$$

Evolution of microstructure

- Porosity evolution: $\dot{f} = (1-f)\dot{\varepsilon}_{kk}^p$
- Void shape evolution: $\dot{w}_i = \alpha_w\, w_i \left(\mathbf{n}^{(3)}\mathbf{n}^{(3)} - \mathbf{n}^{(i)}\mathbf{n}^{(i)}\right) : \dot{\boldsymbol{\varepsilon}}^v, \;\; i = 1,2$
- Void orientation evolution: $\dot{\mathbf{n}}^{(i)} = \boldsymbol{\omega}(\boldsymbol{\Omega}, \dot{\boldsymbol{\varepsilon}}^v) \cdot \mathbf{n}^{(i)}$

Experiments: Butterfly specimen

2D front view

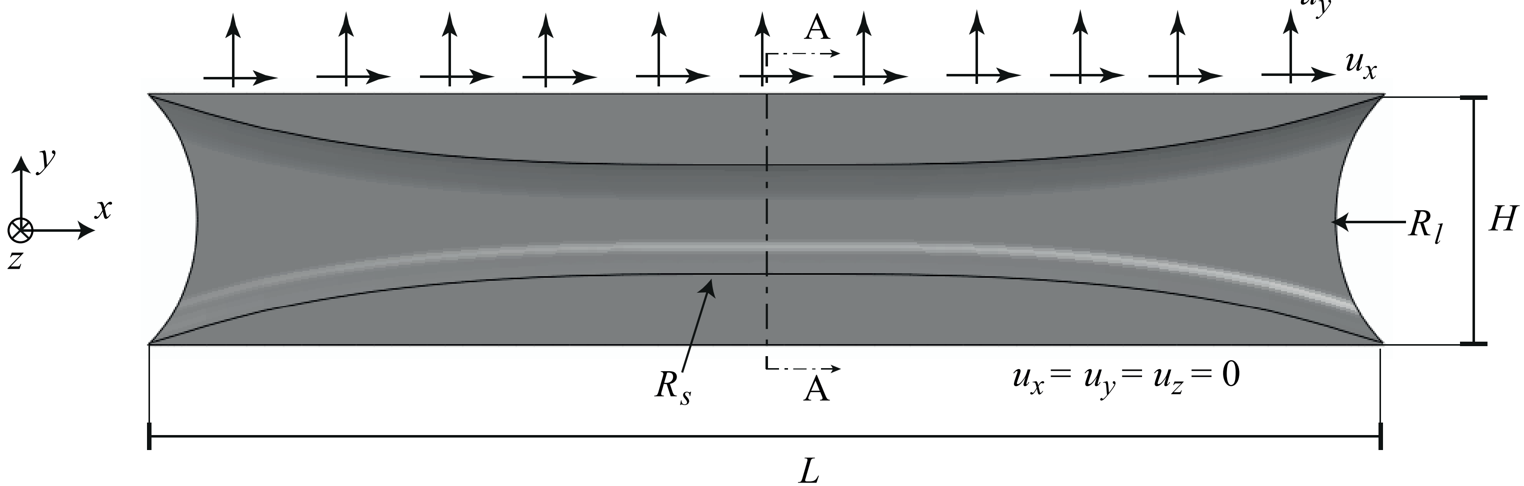

3D view

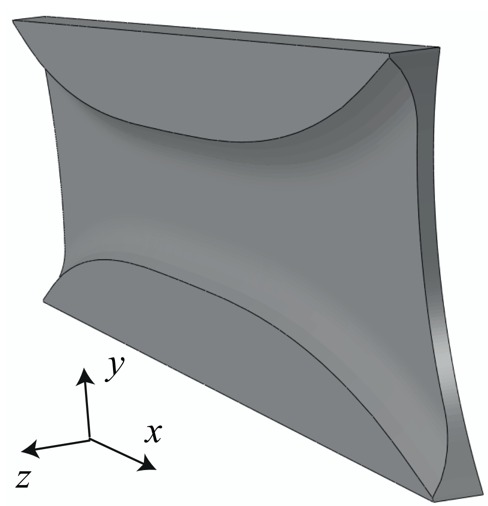

AA section

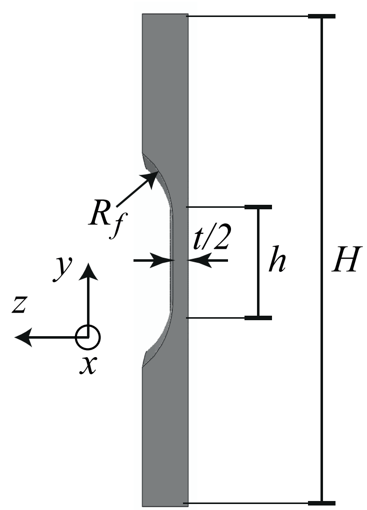

AA section - mesh

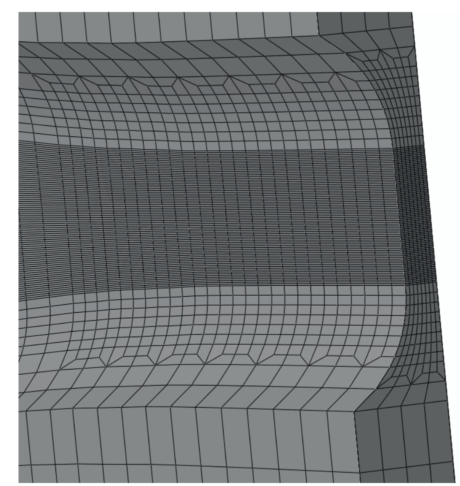

Courtesy of Mathieu Dunand and Dr. Mohr

Macroscopic force-displacement curves

Shear-dominated loading

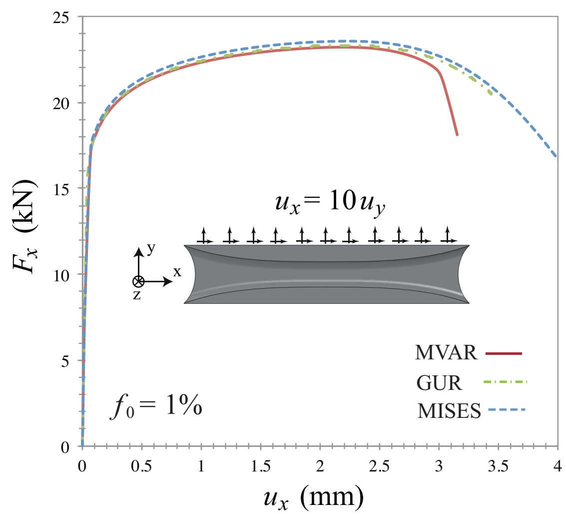

Tension-dominated loading

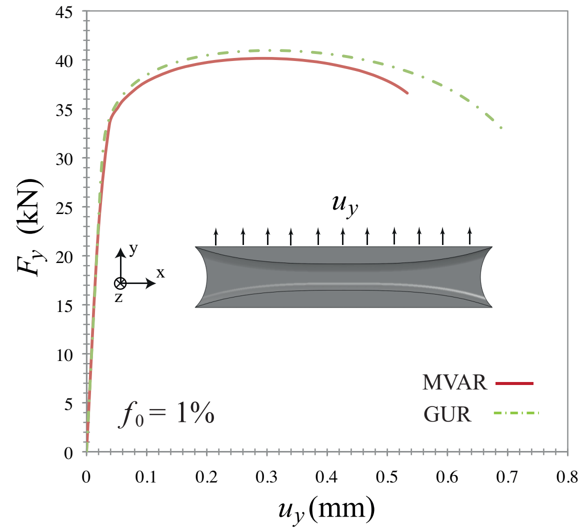

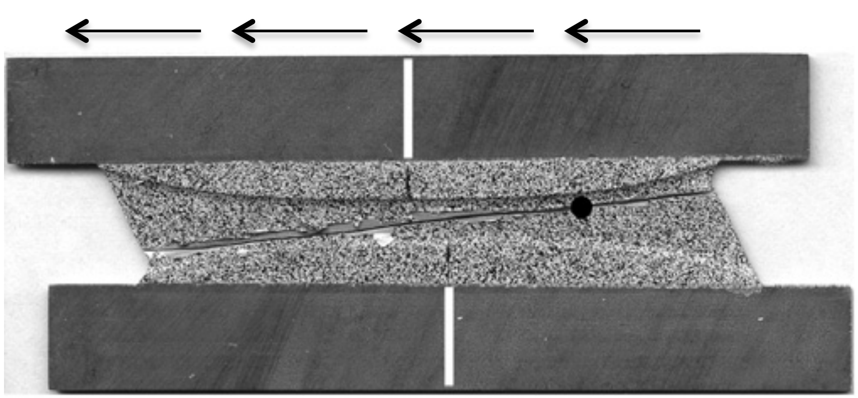

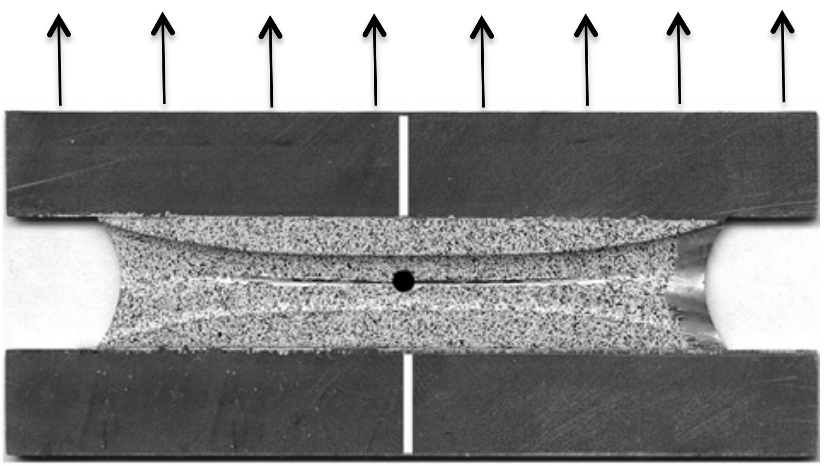

Shear-dominated load: Local fields

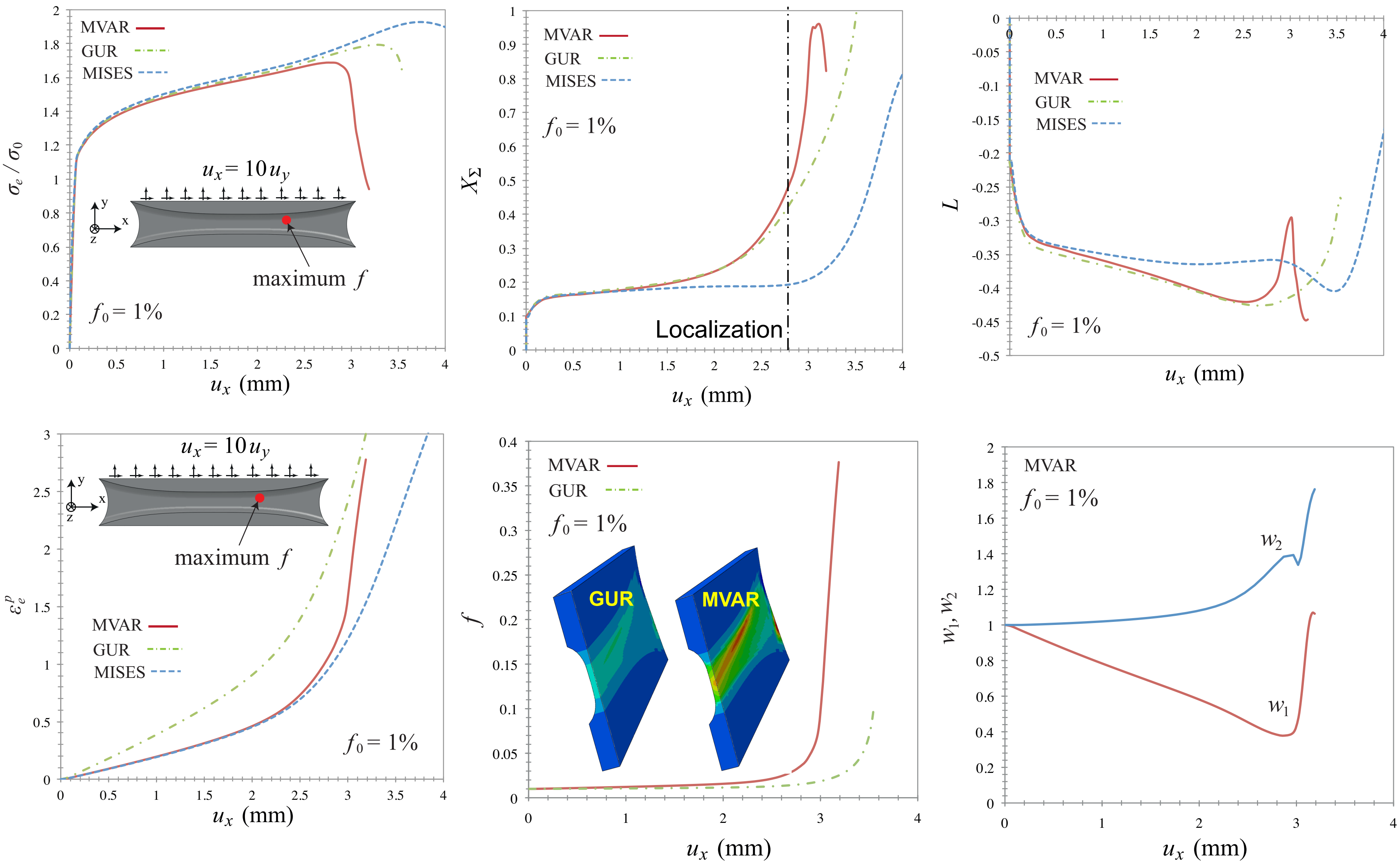

Position of fracture initialization

MISES

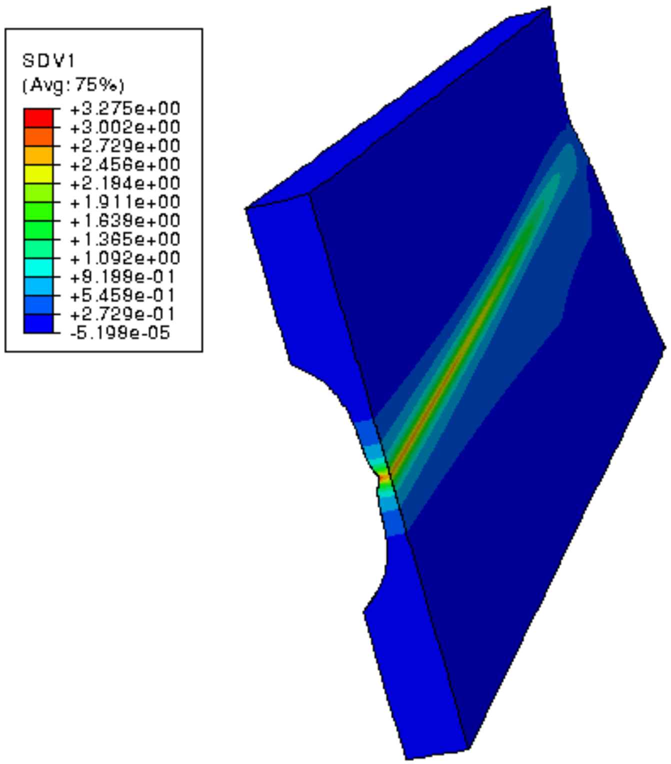

MVAR

GURSON

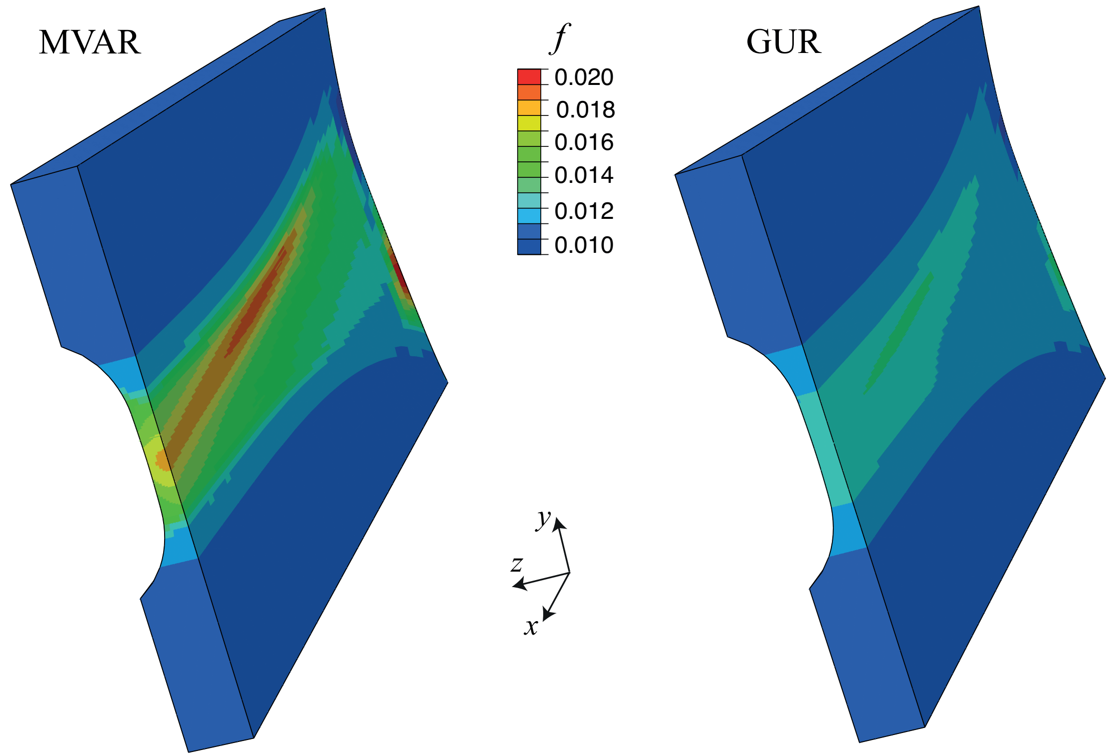

- Plastic strain maps

- Porosity maps

Tension load: Local fields

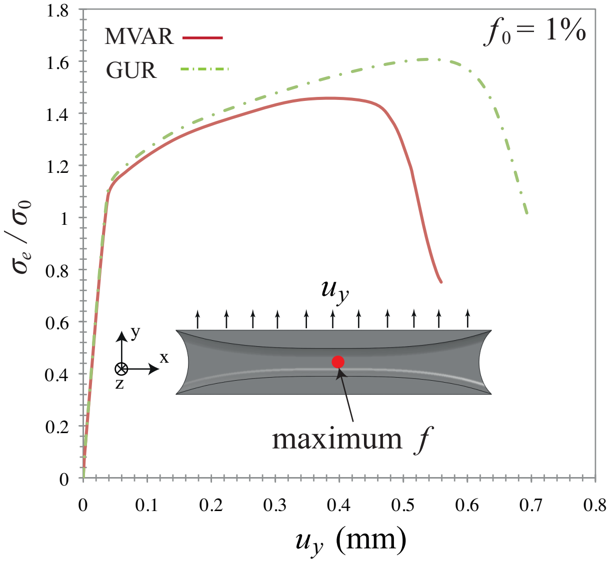

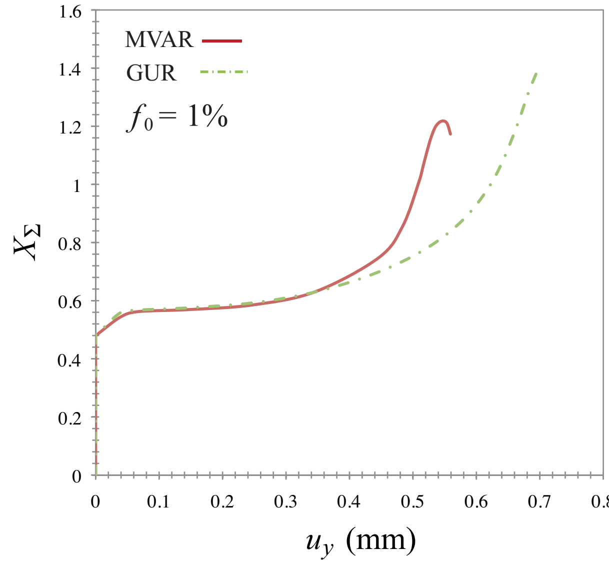

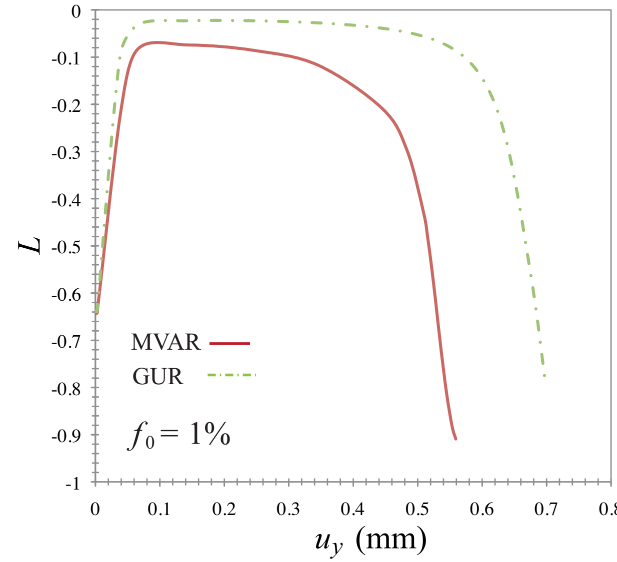

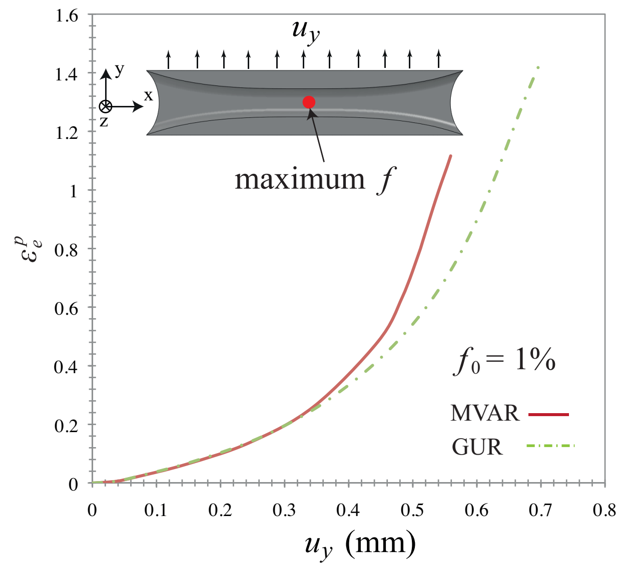

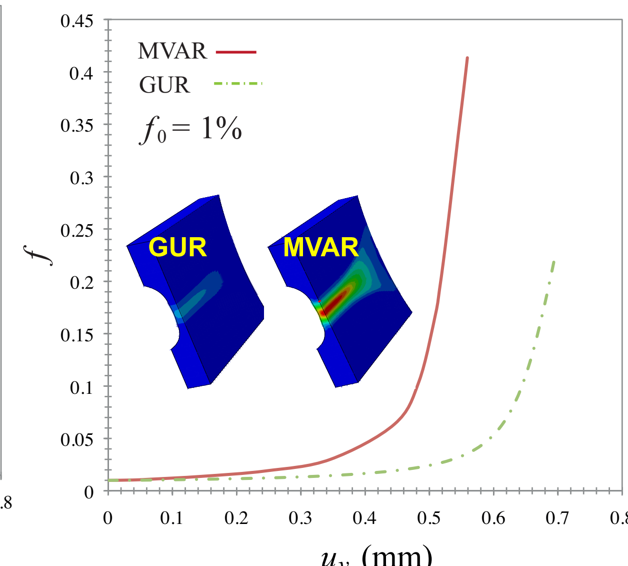

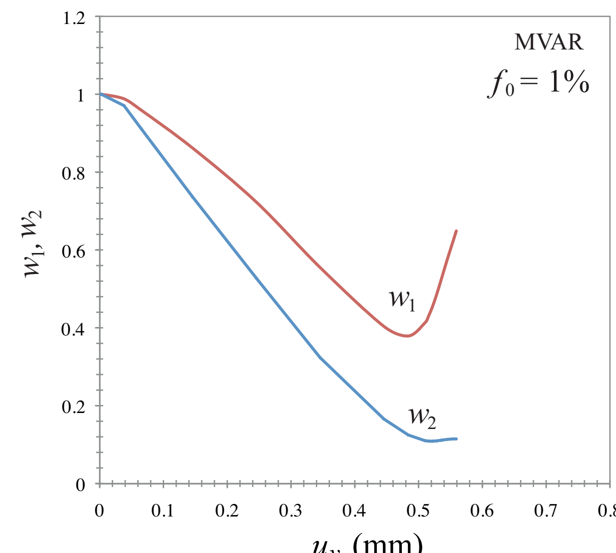

Qualitative comparison with experiments:

Arcan Specimen

Geometry of Arcan Specimen

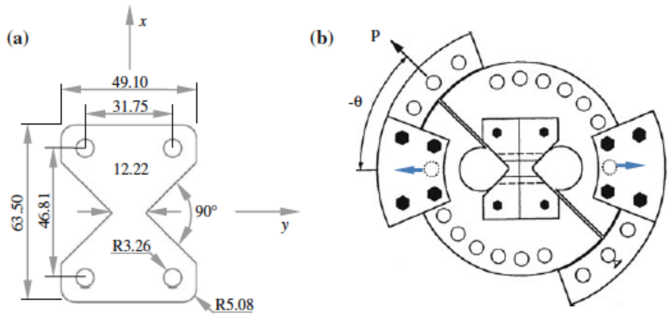

Shearing

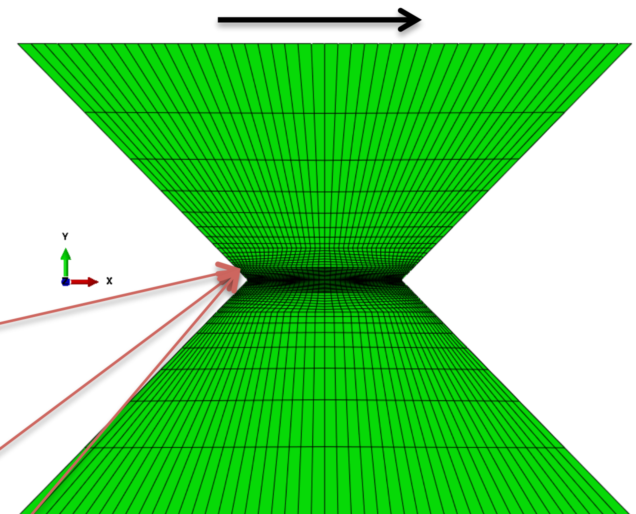

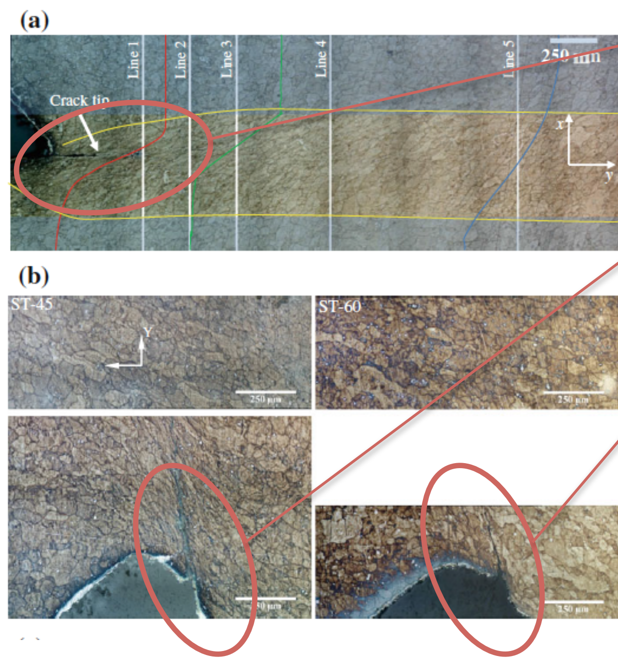

- Fracture occurs above the initial notch
- Very high strains to fracture
- Fracture very localized

Ghahremanineshad and Ravi-Chandar, IJF, 2013

Geometry of Arcan Specimen

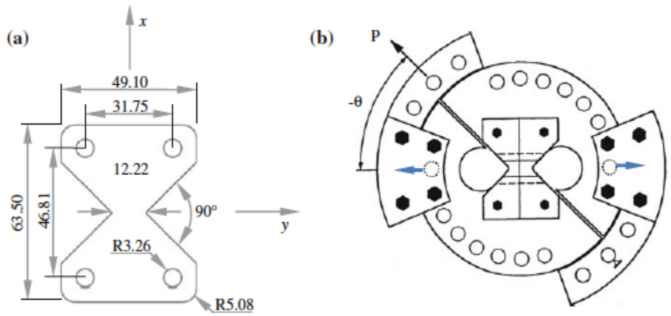

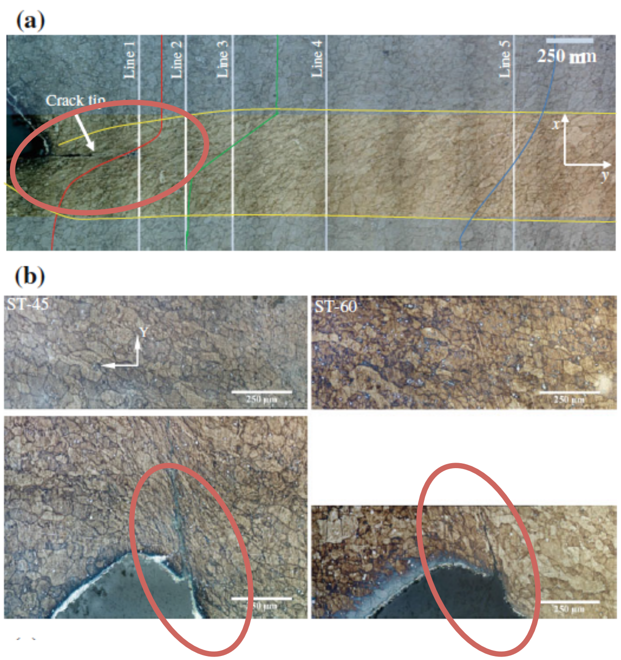

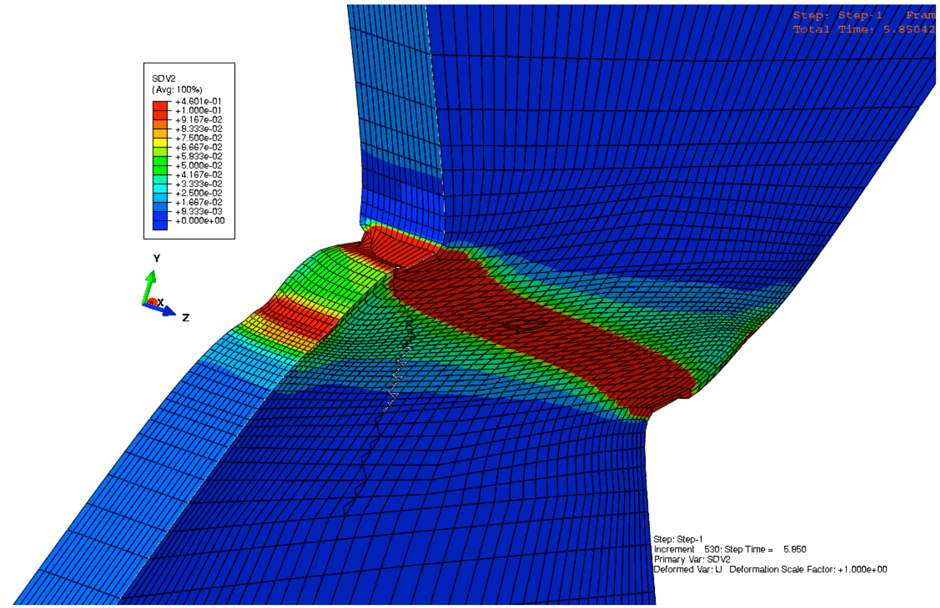

- Fracture occurs above the initial notch
- Very high strains to fracture
- Fracture very localized

Ghahremanineshad and Ravi-Chandar, IJF, 2013

Geometry of Arcan Specimen

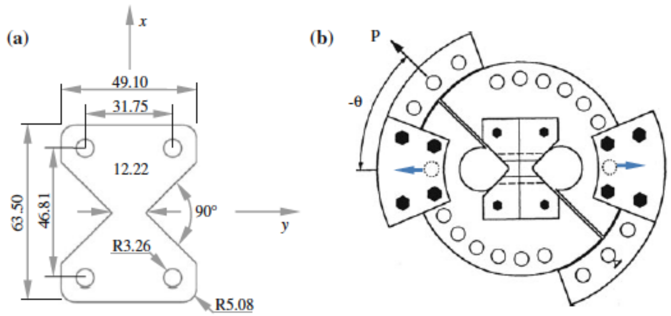

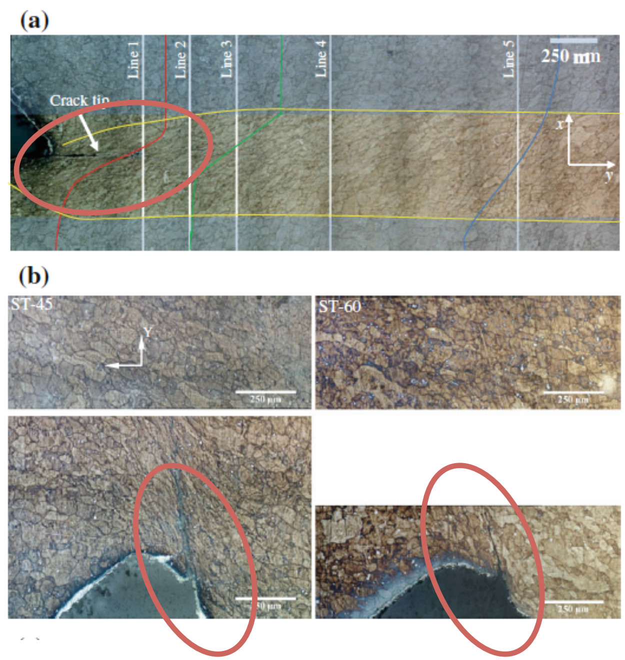

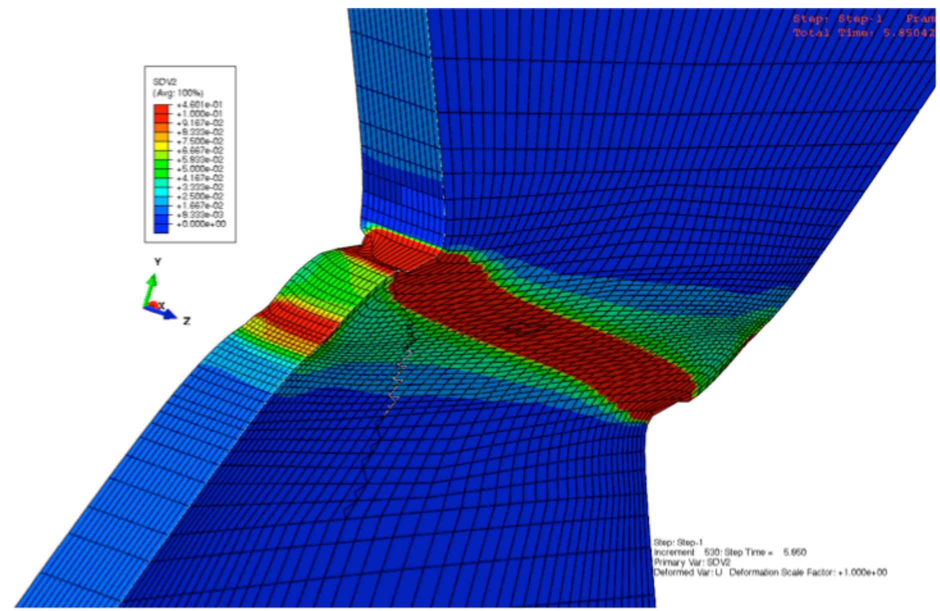

- Fracture occurs above the initial notch
- Very high strains to fracture
- Fracture very localized

Ghahremanineshad and Ravi-Chandar, IJF, 2013

FEM simulations: Qualitative results

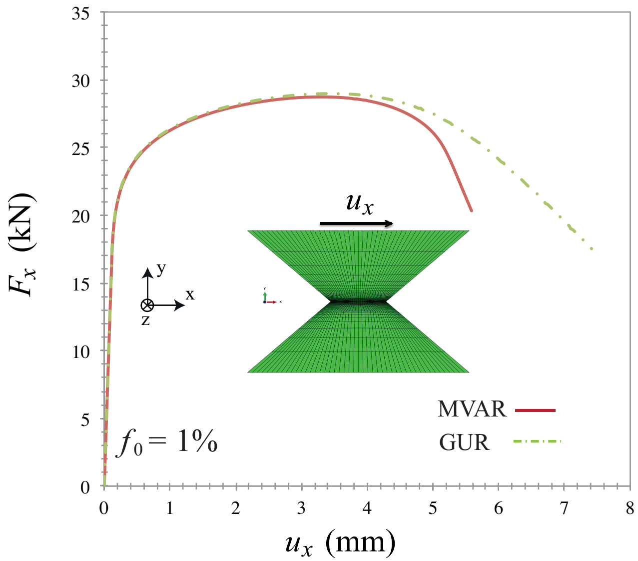

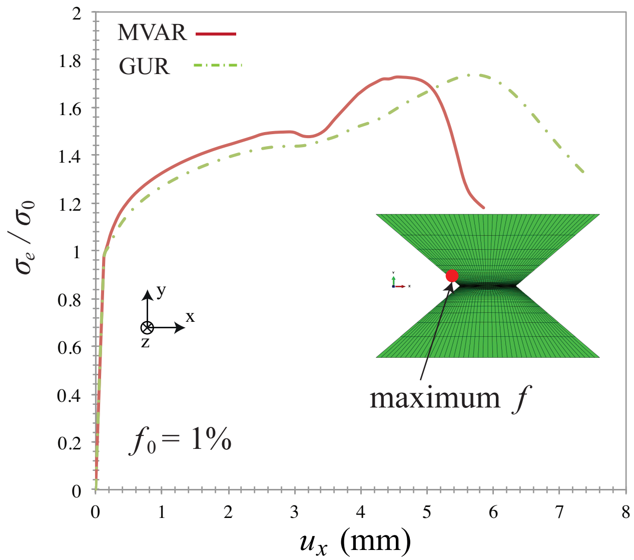

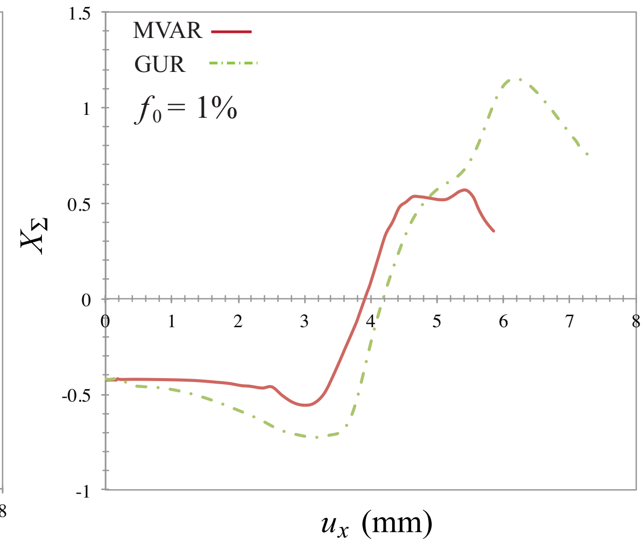

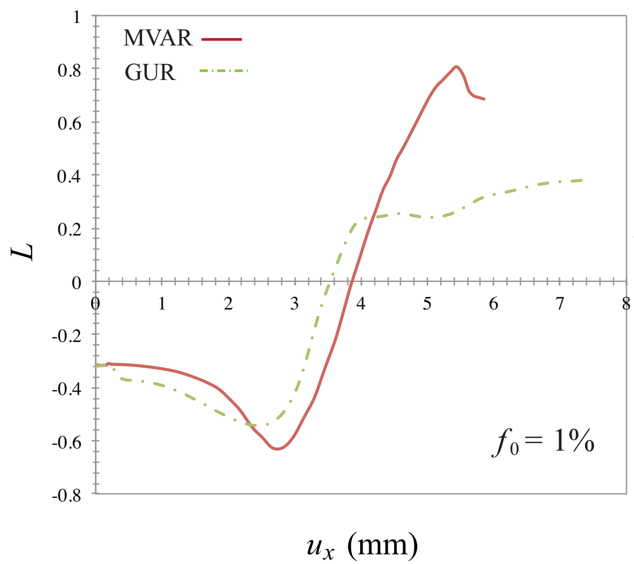

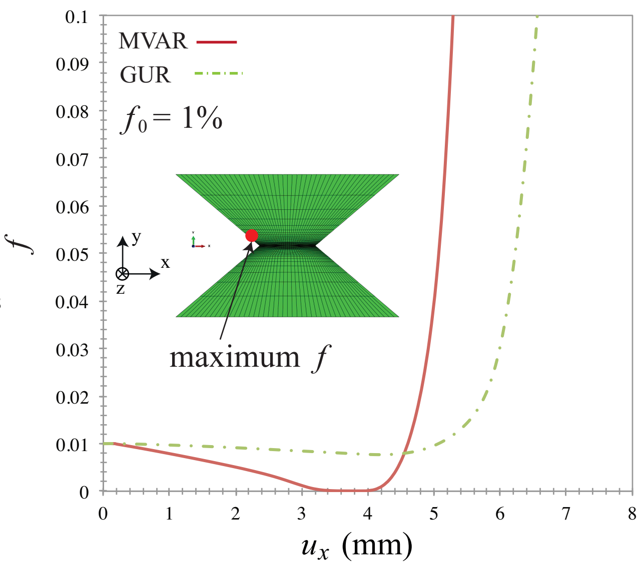

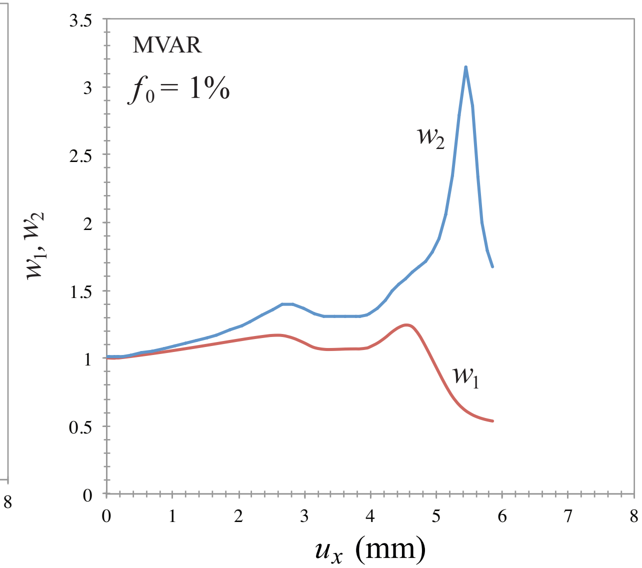

Unpublished Results

Qualitative comparison with experiments: Shear of a Notched Cylindrical Specimen

Large shears : no failure predicted

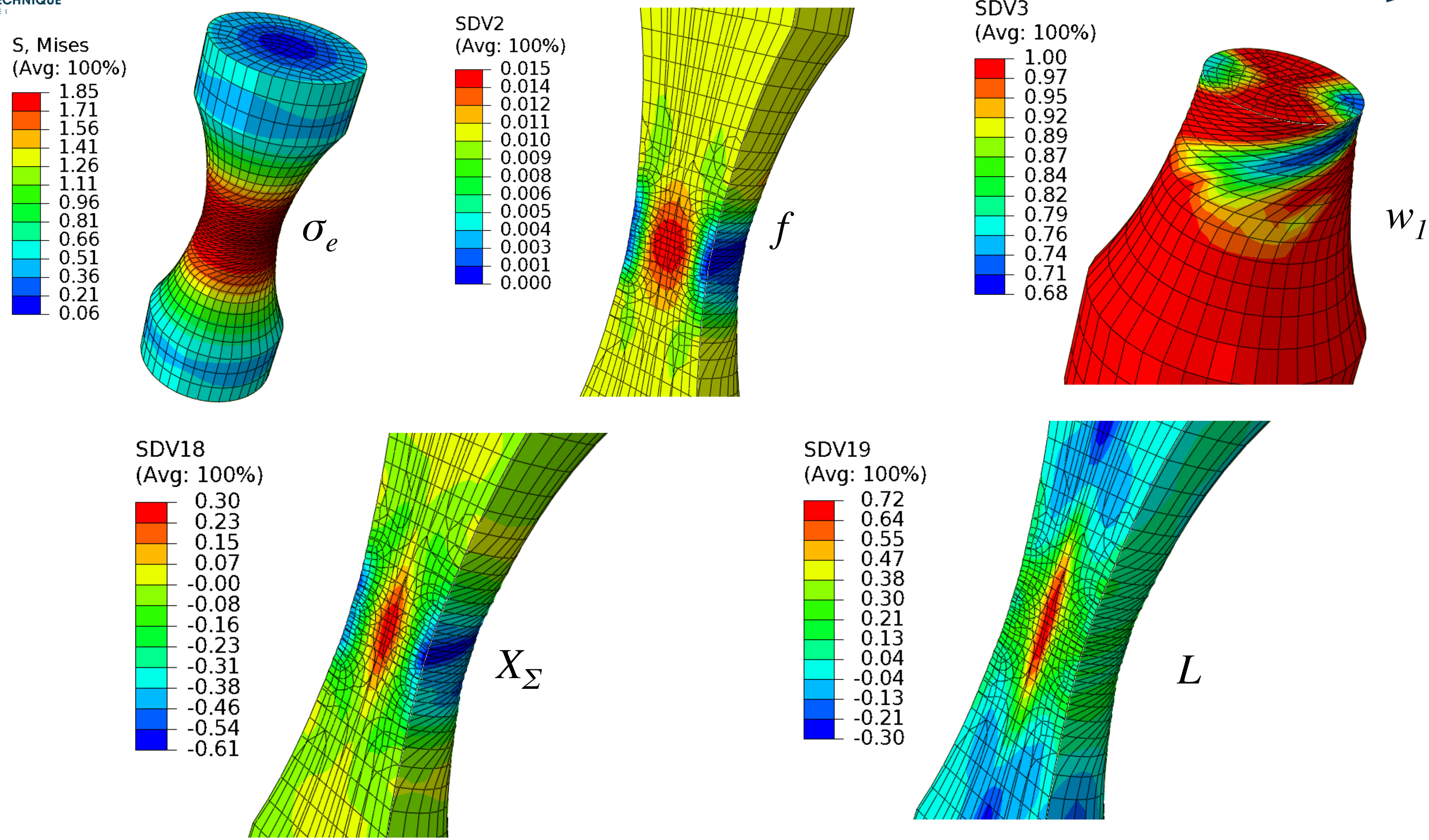

- No failure predicted. Need for additional mechanisms (e.g., damage nucleation, crack nucleation)

Hole expansion test:

Effect of initial void shape due to Forming process

Bore expansion : Geometry and ICs

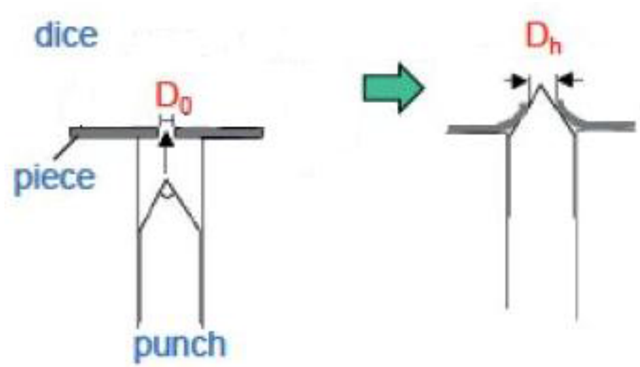

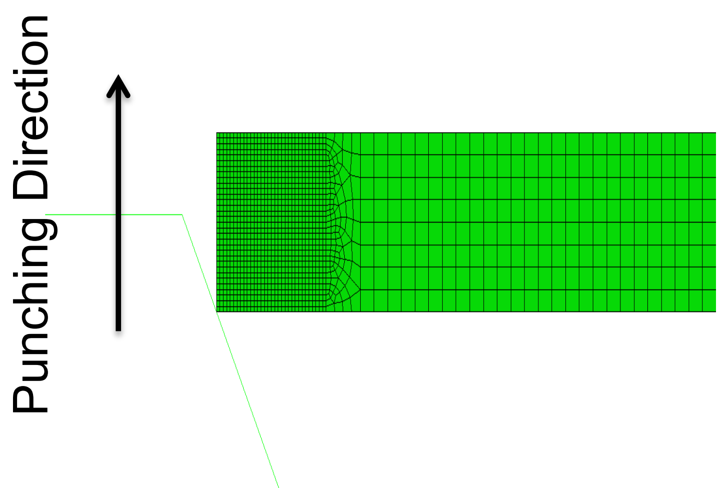

- **Initial Porosity**

$$f_0 = 0.1\%$$

- **Initial Pore Shapes**

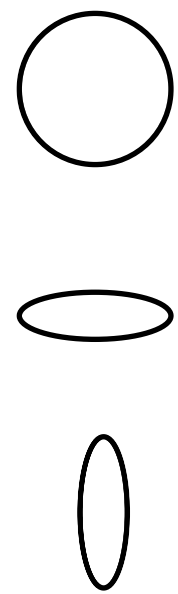

$$w_1 = w_2 = 1$$

$$w_1 = 1,\ w_2 = 5$$

$$w_1 = 1,\ w_2 = 0.2$$

Unpublished Results

FEM simulations: Qualitative results

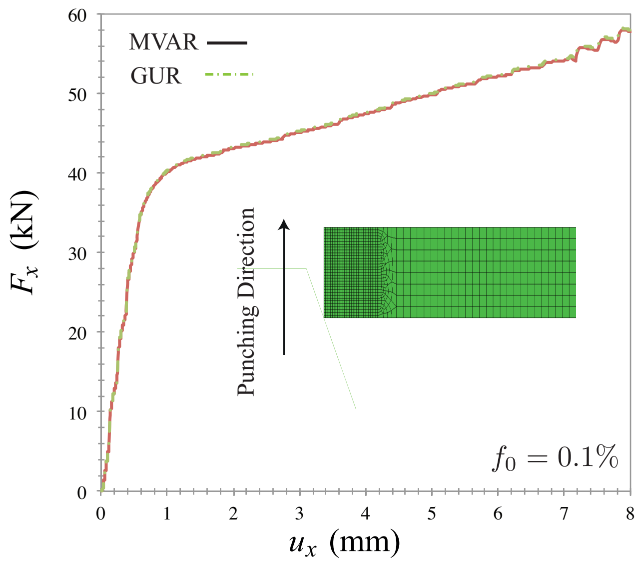

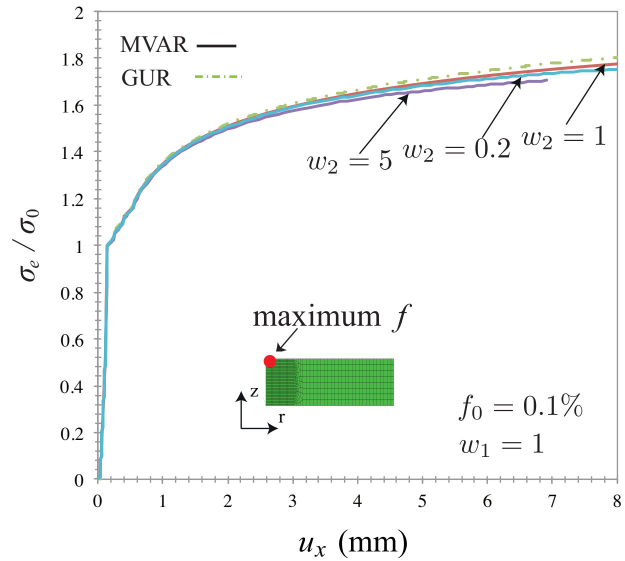

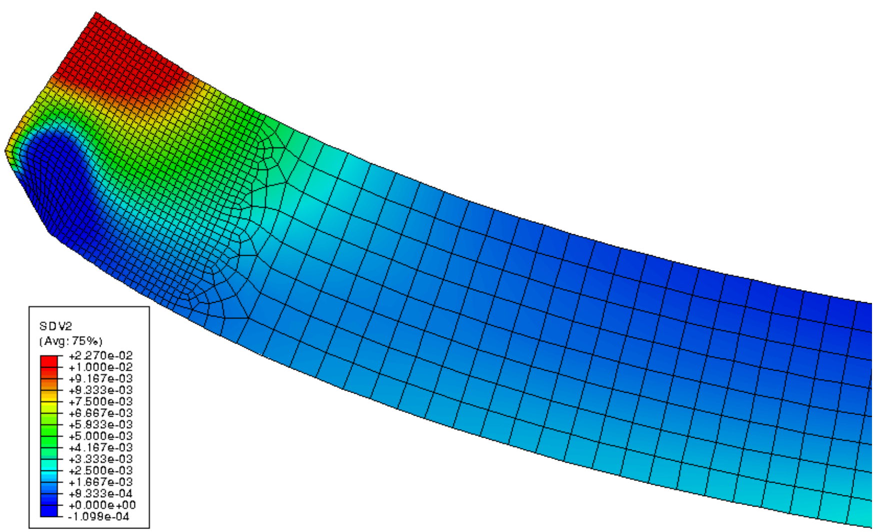

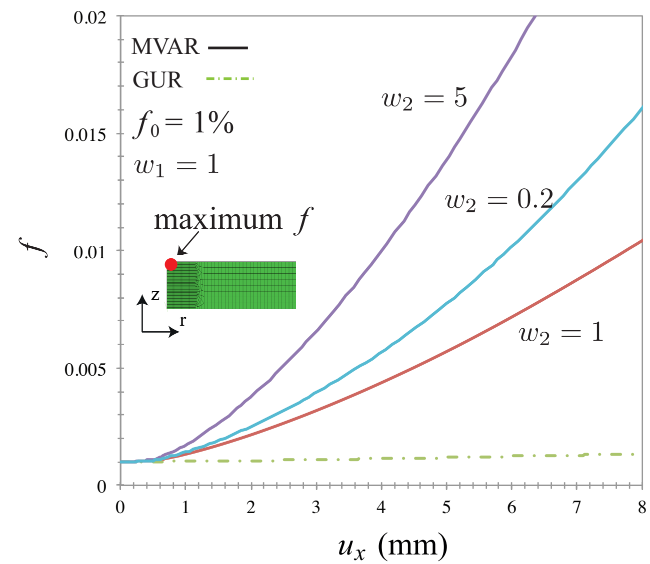

Unpublished Results

Some concluding remarks

- What we see in experiments
  - Fracture and localization is a multi-scale problem
  - At the small scales deformation localization and cracking can co-exist affecting one each other in a non-trivial manner.
  - Pre-existing voids or nucleated ones are a reality?

- Porous material modeling
  - Void shapes and orientations are critical in porous plasticity
  - In crystal plasticity voids lead to non-trivial effects (HCP-basal incompressible)
  - Localization of strains is non-trivial in a random distribution of porosity

- Geometry, loading and materials
  - Geometry, loading and materials are coupled!
  - A sufficiently good plasticity model could tell you if pores are the source of failure or not!
  - Stress fields depend on the use of the model (check Strain triaxiality)

THANK YOU FOR YOUR ATTENTION

- Laboratory of Solid Mechanics (LMS)
  - http://www.lms.polytechnique.fr

- Kostas Danas webpage
  - http://hera.polytechnique.fr/users/kdanas

- Ecole Polytechnique
  - http://www.polytechnique.edu

- National Center of Scientific Research (C.N.R.S) webpage
  - http://www.cnrs.fr/index.php

Some concluding remarks

Modified VAR model

- Simple modification of the earlier variational method.
- Easily implemented in FEM and very stable numerically
- Time of calculations in the order of Gurson model
- Includes shape and rotation effects ab initio
- x Does not have the character of a bound any more

MVAR & Experimental geometries

- Even for a low triaxiality macroscopic load the mode of structural failure is driven by geometrical aspects leading to high triaxiality locally and void growth.
- MVAR and GUR exhibit significant quantitative differences at the local level.
- Qualitatively, MVAR tends to localize more abruptly than GUR (similar to the experiments), but differences are very small until that localization point.
- The evolution of the void shape leads in general to more criticalbehavior, which in turn leads to faster material & geometrical failure locally.

Grpahical Yield Surface 3D

Meridional plane : $\sigma_e - \sigma_m$

Π – plane : $\sigma_e - \theta$

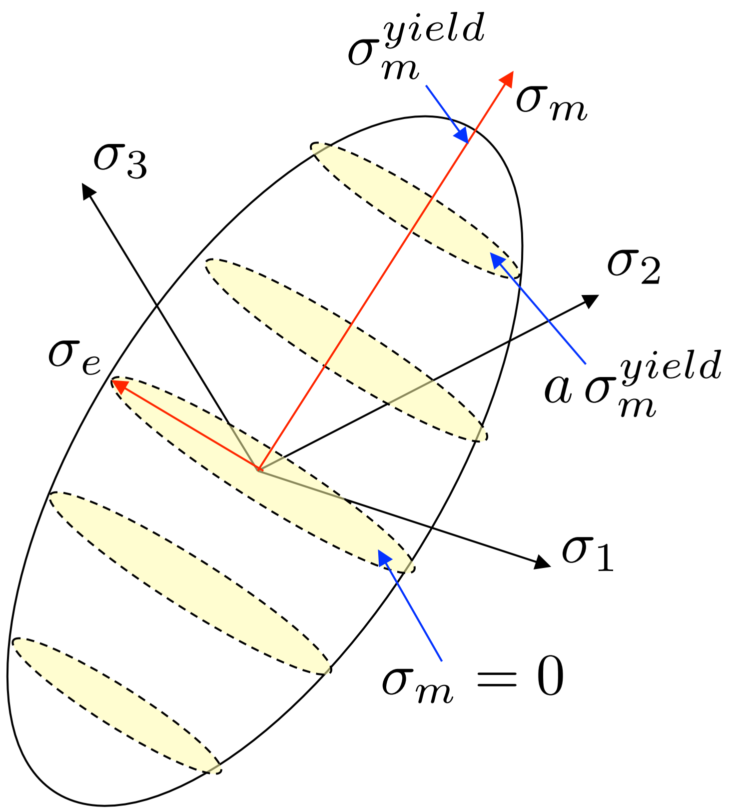

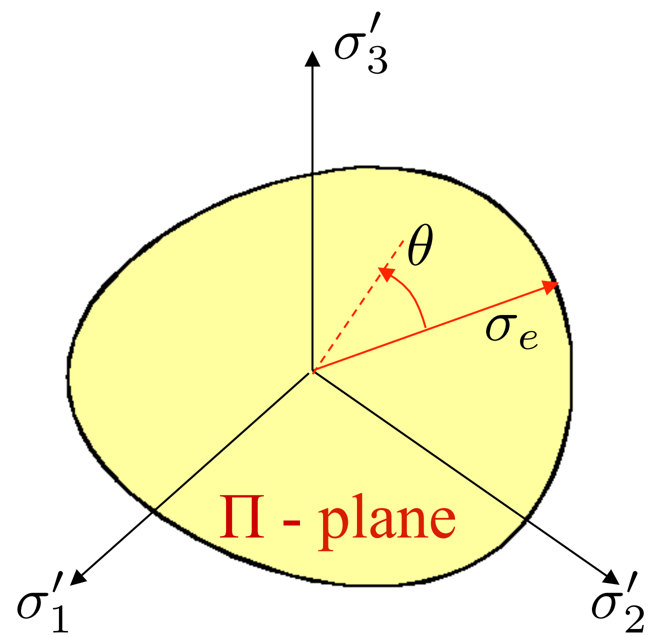

Lode angle θ is the polar angle in the Π - plane

Ponte Castañeda (2002), Aravas & Ponte Castañeda (2004), Danas & Ponte Castañeda (2009)

Effect of void shape in FCC

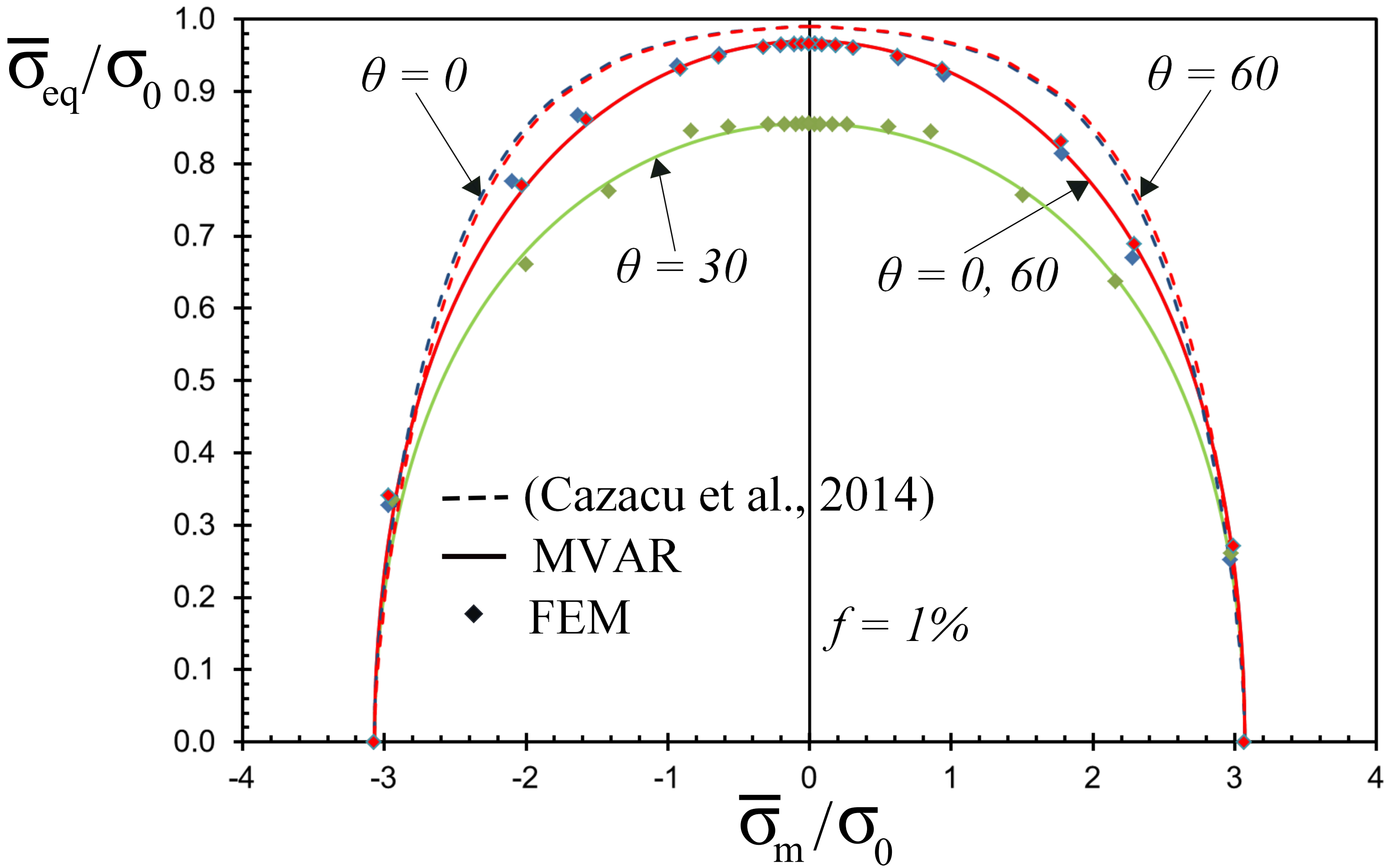

Void shapes in HDPE

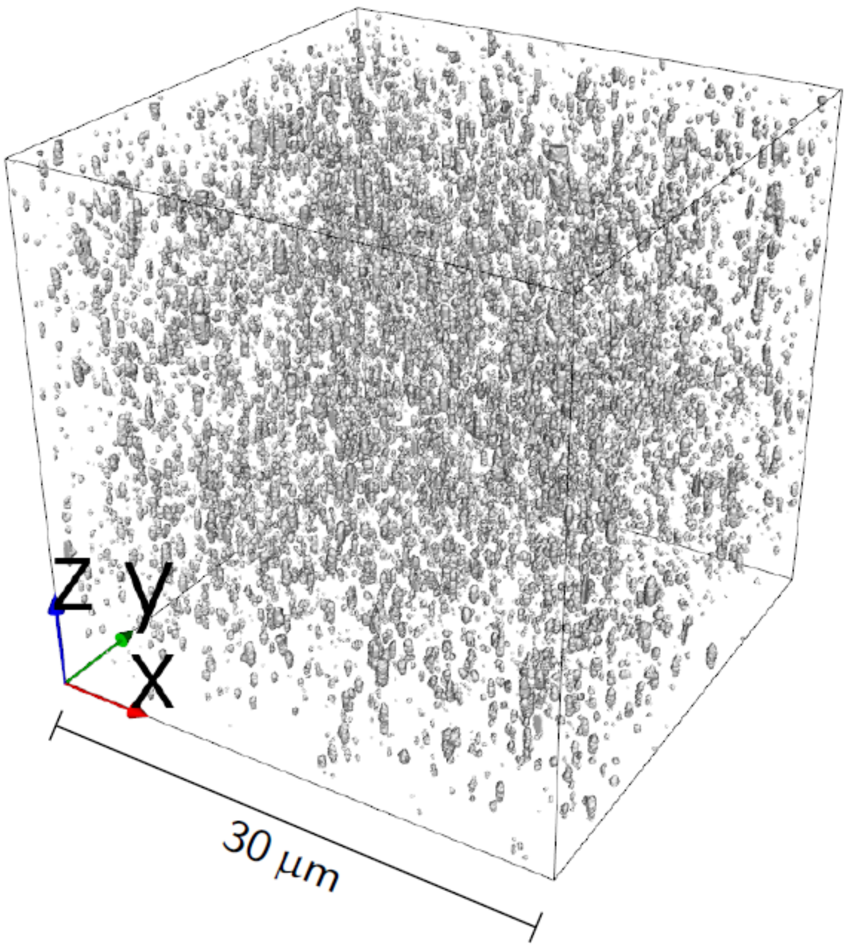

(a)

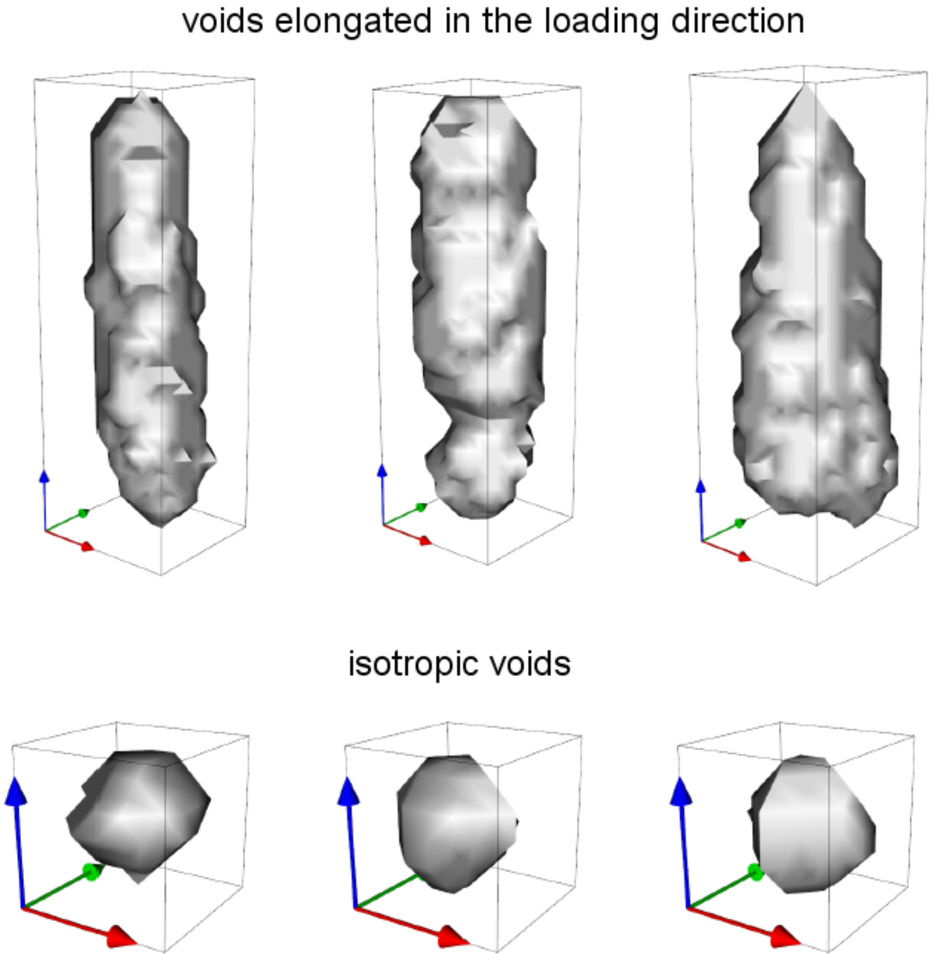

(b)

Evolution of voids: ductile crack opening

Al-Cu-Mg, AA2139 alloy

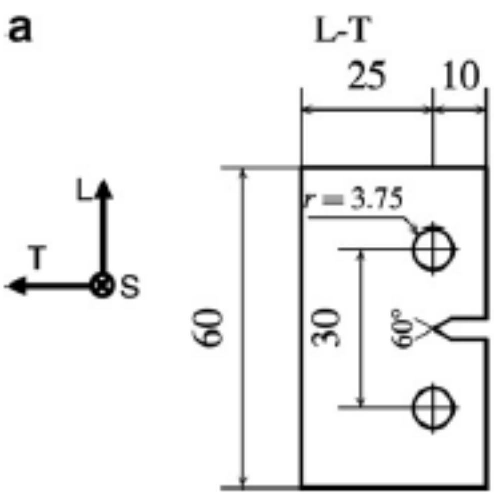

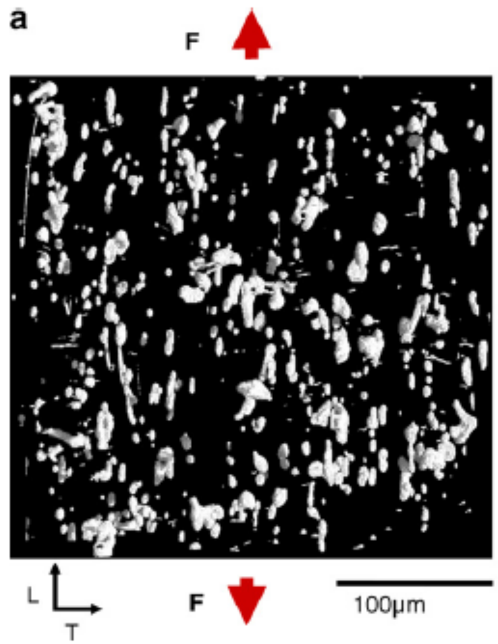

- 3-D void distribution and morphology in the L-T plane
- Volume of 350x350x180µm
- Void content appears higher due to projection

- 3-D close up of coalescing elongated voids in the L-S plane in one column
- Significant void shape evolution

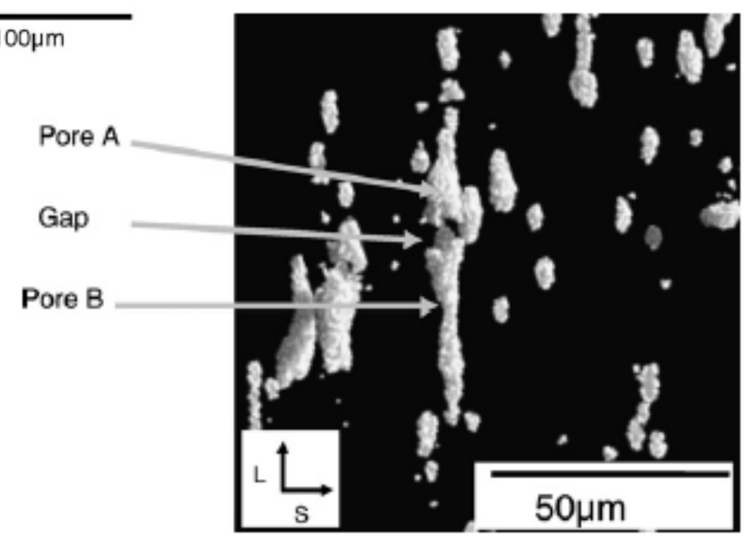

[Morgeneyer et al., 2008]

Tresca Yield functions (Bonus CP)

Modified VAR (MVAR)

(Mbiakop, Constantinescu, Danas, in preparation)

Spherical voids: Effect of Lode angle

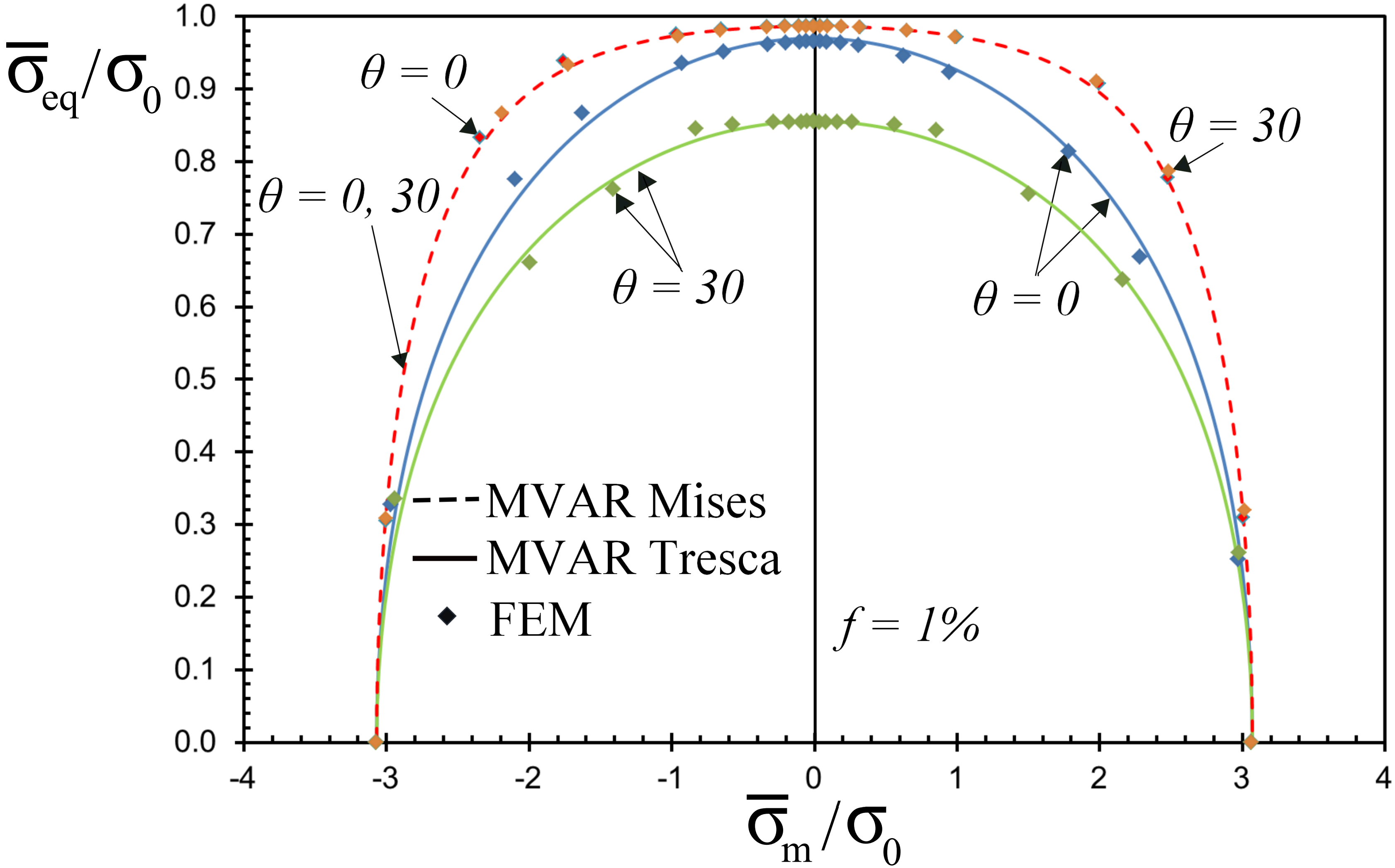

Void shape effect

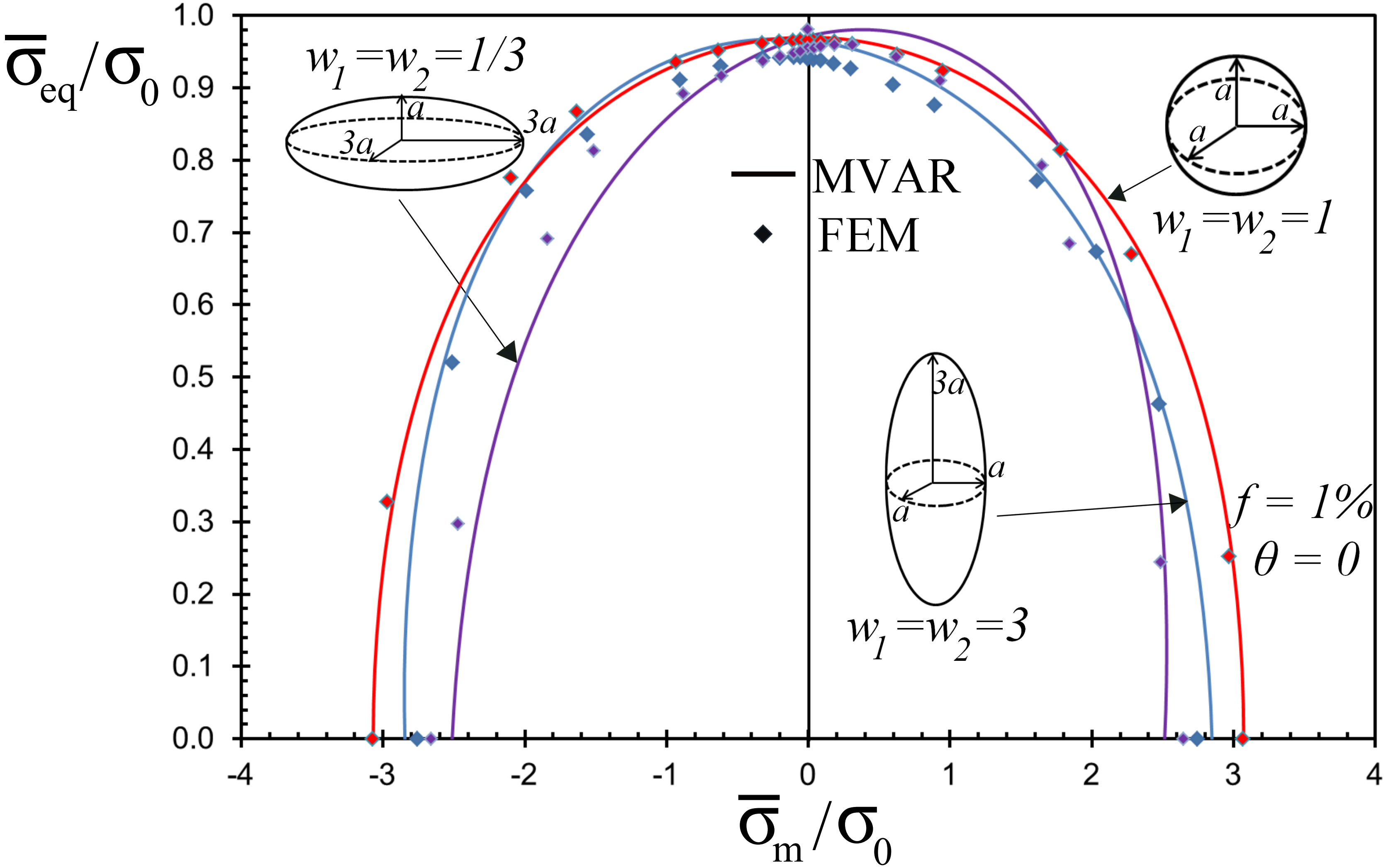

Material parameters & Initial Conditions

- Elastic material properties

$$E = 1000\,\sigma_0,\ \nu = 0.3,\ \varepsilon_0 = \sigma_0/E$$

- Hardening exponent *N*

$$\sigma_y = \sigma_0 \left(1 + \frac{\varepsilon^p}{\varepsilon_0}\right)^{1/N} \quad \text{with} \quad \varepsilon^p = \int_0^t \dot{\varepsilon}^p_{eq}\,\mathrm{d}\,t$$

$$N = 5, 10, 20, 100$$

present work

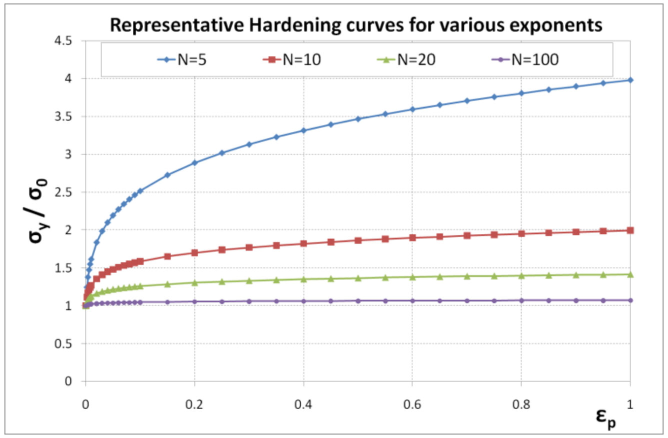

- Initial values for the microstructural variables (initially isotropic)

$$\varepsilon^p = 0,\ f_0 = 1\%,\ w_1 = w_2 = 1 \quad \text{at time} \quad t = 0$$

Standard Stress measures

- Stress triaxiality: $\boxed{X_s = \sigma_m / \sigma_e}$ $\quad \sigma_m = \sigma_{kk}/3, \;\; \sigma_e = \sqrt{3\,\sigma'_{ij}\,\sigma'_{ij}/2}$

- Lode angle : $\boxed{L = -\cos 3\theta = -\dfrac{27}{2}\det\left(\dfrac{\sigma'_{ij}}{\sigma_e}\right)}$ $\quad \begin{cases} 0 \leq \theta \leq \frac{\pi}{3} \\ -1 \leq L \leq 1 \end{cases}$

- IMPORTANT NOTE: In the presented models (MVAR, VAR, SOM) the response is anisotropic and depends on the entire stress tensor in general loadings